Surface Ozone Distribution & Trends Over Ireland: Insights from long-term measurement record and source attribution modelling

Nikhil Korhale [1], Tabish Ansari [2], Tim Butler [2], Jurgita Ovadnevaite[1], Emmanuel Chevassus[1], Darius Ceburnis[1], Damien Martin[1,] Colin D. O'Dowd[1], Liz Coleman[1]

1 School of Natural Sciences, Physics, Ryan Institute's Centre for Climate & Air Pollution Studies, University of Galway, Galway, Ireland

2 Research Institute for Sustainability - Helmholtz Centre Potsdam, Potsdam, 14467, Germany

Corresponding author:

Name - Dr. Liz Coleman

Email Id – liz.coleman@universityofgalway.ie

Abstract

We present an analysis of long-term trends in surface ozone (O_3) across Ireland, with specific focus on the Mace Head atmospheric research station, representative of Northern hemispheric background atmospheric conditions. Surface O_3 dataset was characterised using advanced trajectory analysis and seasonal decomposition, revealing distinct seasonal and spatial patterns. Findings show a significant rising trend in surface O_3 at Irish urban sites over the past two decades but without a similar trend at coastal sites. Highest O_3 levels and exceedances were observed at remote coastal sites, which are less susceptible to influence from local and easterly emissions but heavily influenced by transboundary pollution and stratospheric intrusion.

At Mace Head, springtime O_3 levels exhibit a declining trend, whereas wintertime levels show a rising trend. Focussing on the clean sector, the springtime decline remains significant, but without corresponding clean sector rising wintertime trends, implying the rising winter trends occur in response to declining local, United Kingdom (UK) and European emissions. Advanced modelling tools are used to quantify O_3 source contributions, elucidating key drivers behind the observed changes. Characteristic springtime O_3 maxima at Mace Head are predominantly attributed to stratospheric transport, hemispheric and long-range transport and lightning NO_x. The complementary trend and sectoral observational analysis reveal a decline in total spring-time concentrations, with a more rapid decline in exceedances from the UK & continental sector.

This research highlights the importance of seasonal factors in air quality management across Ireland, emphasising the need for a multi-faceted approach to control O_3 levels and reduce exceedances through global and regional emission reductions.

Keywords – Ozone, Trends**,** Meteorology, NO_x, Climate, CH_4, Emissions.

1. Introduction

Surface Ozone (O_3) has significant implications for health, vegetation, and climate. Its chemical production is driven by complex photochemical processes, responding non-linearly to pollution control, creating challenges for its effective regulation. Elevated O_3 levels cause severe health issues with prolonged exposure to high O_3 levels, causing respiratory issues, cardiovascular problems, and reduced lung function, particularly in sensitive populations such as children, the elderly, and individuals with pre-existing respiratory conditions (Lin et al., 2018; Todorović et al., 2019; Zhang et al., 2019, WHO, 2021). O_3 pollution can adversely impact vegetation by reducing agricultural productivity (Ashmore et al., 2005; Paoletti et al., 2006). O_3 is also the third most significant greenhouse gas after Carbon Dioxide (CO_2) and

methane (CH_4), contributing to climate instability (IPCC, 2021). O_3 can live for several weeks in the free troposphere, and it is transported by large-scale atmospheric circulation patterns (Wespes et al., 2017). Meteorological factors such as temperature, solar radiation, wind speed, and atmospheric stability play a significant role in O_3 formation. (Ding et al., 2023; Khiem et al., 2010).

O_3 is formed in the atmosphere from precursors Nitrogen Oxides (NO_x), carbon monoxide (CO), and volatile organic compounds (VOCs) through photochemical reactions. Photochemical production requires solar radiation, and reaction rates are correlated with temperature, it is noted that little photochemical production occurs at temperatures below 20°C (Coates et al., 2016). The reactive, interdependent atmospheric chemistry leads to a non-linear relationship between O_3 and its precursors (Seinfeld and Pandis, 2016), and effective O_3 mitigation requires a comprehensive understanding of processes influencing O_3 production and removal mechanisms (Fowler et al., 2013).

NO_x can suppress or enhance O_3 formation, depending on the local atmospheric chemistry regime. In polluted urban environments, high NO_x emissions can lead to O_3 dissociation, retarding photochemical O_3 formation (NO_x-saturated/VOC-limited regime), with local pollution events potentially titrating surface O_3 completely, converting NO to NO_2. This effect is more prevalent in wintertime, when temperatures are low, and there is little solar radiation to facilitate photochemical production of O_3.In relatively clean environments, O_3 formation is correlated with NO_x concentration (NO_x-limited regime) (Tavella & da Silva Júnior, 2021).

O_3 and precursors can be transported over great distances in the troposphere, with transport from distant polluted regions accounting for 40% of O_3 abundance in remote regions (Sudo and Akimoto, 2007). While O_3 is transported in air masses from distant sources, although titration occurs, O_3 is replenished via mixing. Over Ireland, advection of O_3 rich air from continental outflow is a significant source of Irish O_3, but European continental air-masses can also

transport pollutants to trigger O_3 depletion events, but the O_3 depleting effect of the air masses originating from Europe is in decline in response to European Union (EU) pollution control strategies (Derwent et al., 2024).

Seasonal and regional variations further complicate the regulation, with higher O_3 levels observed in summer across the northern hemisphere due to increased temperatures, solar radiation, and abundant precursors (Moiseenko et al., 2021; Sicard et al., 2016). In marine boundary layers, O_3 levels are generally lower than in continental regions, though specific oceanic environments can exhibit high O_3 concentrations due to inflows from polluted areas (Boylan et al., 2014; Girach et al., 2020). Another factor which influences O_3 levels is the North Atlantic Oscillation (NAO), which influences O_3 levels in Western Europe. During a positive NAO phase, O_3 levels increase. In contrast, during a negative NAO phase (NAO-low), O_3 levels decrease. This effect is particularly notable in southwest, central, and northern Europe (Bonaccorso et al., 2015; Creilson et al., 2003; Pausata et al., 2012).

While Ireland's air quality is mostly governed by the influx of clean maritime air from the Atlantic Ocean (Tripathi et al., 2010), certain synoptic scenarios allow for the intrusion of polluted air masses from continental Europe. These events, though infrequent, can bring substantial amounts of O_3 and its precursors (NO_x and VOCs), contributing to short-term O_3 pollution episodes.

The World Health Organisation (WHO) publishes Air Quality Guidelines (AQGs) as a non-legally binding global target for governments to achieve within their jurisdictions. These AQGs comprise evidence-based recommendations of limit values to protect public health. The current recommended AQGs for O_3 is expressed as a daily maximum of 8-hourly running average O_3 value of 100 $\mu g/m^3$. Days when O_3 levels exceed the recommended AQGs are classified as exceedance days. Factors contributing to exceedances include high solar radiation, stagnant air masses, and local emissions and regional and transboundary transport of O_3 and precursors.

Globally, over the past 150 years, there has been a 40% increase in O_3 levels owing to rising precursor emissions. (Archibald et al., 2020; Griffiths et al., 2021; Young et al., 2013). Despite emission reduction policies, O_3 pollution remains a problem, with over 94% of those living in European cities exposed to O_3 levels exceeding the WHO AQGs in 2022 (EEA, 2024; World Health, 2021). Over 22,000 premature deaths in the EU were attributable to short-term exposure to O_3 in 2021(Soares et al., 2023).

Long-term O_3 measurement data from the Mace Head research station in Ireland reveal a distinct seasonal pattern with peaks during spring and lows in summer. (Derwent, 1998; Derwent et al., 1994, 2018). Historical trends show increasing baseline O_3 levels in the 1980s and 1990s, stability in the 2000s, and a decline in the 2010s.(Derwent et al., 2013; Derwent, Manning, Simmonds, Spain, et al., 2018). Recent observational and modelling data have identified a broad O_3 maximum in spring and early summer, aligning with peak stratospheric transport (Ansari et al., 2024; Lin et al., 2012; Russo et al., 2023). O_3 dynamics are complex, and studies reveal discrepancies between model output and observations. (Bessagnet et al., 2016; Vautard et al., 2012), highlighting the need for further understanding of factors governing O_3 levels and trends.

This study investigates the distribution and trends of O_3 and its precursors across Ireland, providing valuable insights into the regional and hemispheric impact on Irish surface O_3 levels and exceedances. We analyse the long term O_3 observational dataset for Ireland, identifying the mean and range of O_3 levels and seasonal variation at each site. We identify the long-term annual and monthly trends at each site, quantifying the significance of each trend according to TOAR guidelines (Chang et al., 2023). We also identify the frequency and seasonality of exceedance of the WHO AQGs for the protection of human health from O_3 pollution for each site. The trends and seasonality are contextualised by looking at trends in the Irish instrumental record of dominant precursors of NO_x and CH_4 and we discuss the relationship between NO_x

and O_3 by comparing anomalies between monthly average NO_x and O_3 during lockdown compared to the average values for the three years prior to lockdown. Advanced modelling results using the global Tropospheric Ozone Attribution of Sources with Tagging 1.0 (TOAST 1.0) framework (Butler et al., 2018; Butler et al., 2020) are validated against measurements at various sites for simulation period 2000-2018, and the simulation results analysed to determine the geographical and sectoral source of precursors that contribute to simulated O_3 at Mace Head, identifying seasonality and long-term trends in the sources. Finally, the observational data are classified using advanced trajectory clustering methods to separate air masses from the clean sector from those influenced by local, UK or EU emission sources, with seasonal trends identified for both clean and polluted sectors, and the exceedances classified as coming from either the clean or polluted sector.

This research highlights significant seasonal and temporal variations and long-term trends in O_3 concentrations, and the integrated approach, including observational and modelling analysis, enhances our understanding of the drivers of O_3 concentrations, trends and exceedances over Ireland and allows quantification of global and regional contributions to Irish surface O_3.

2. Data and methodology

2.1 Observational Network and Analysis Approach

Measurement data is obtained from the Environmental Protection Agency, Ireland (EPA) (https://eparesearch.epa.ie/safer/). The O_3 monitoring network shown in Figure 1 has been operational in Ireland since 1994. O_3 is measured using an API M400 and an O_3 analyser based on UV photometry at all EPA monitoring sites. At the Mace Head site, O_3 was measured using a Monitor Labs 8810 analyzer and a Thermo Environmental O_3 monitor. Measurement

operating accuracy is within 1.0 ppb, based on precision, calibration and drift characteristics. Measurements of O_3 precursors from EPA air quality monitoring sites are also monitored. The details of the measurement sites are shown in Table 1. Numerous previous studies have analysed this data, with a particular focus on the analysis of Mace Head data to assess background O_3 (Carslaw, 2005; Derwent, 1998; Derwent et al., 1994, 1998, 2001, 2004, 2008, 2013; Derwent, Manning, Simmonds, & Doherty, 2018; Derwent, Manning, Simmonds, Spain, et al., 2018; Oltmans et al., 2013; Simmonds et al., 2004; O. P. Tripathi et al., 2010, 2012, 2013). CH_4 data is obtained from the Integrated Carbon Observation System (ICOS) network, accessible at https://www.icos-cp.eu/data-products/ATM_NRT_CO2_CH4.

For this analysis, the observational sites were classified into three categories: Coastal, Rural, and Urban, as shown in Figure 1. The classification of the sites is based on Spohn et al., 2022, with the addition of the coastal category. Hourly data were used to evaluate annual trends based on monthly mean concentrations. Seasonal analysis conducted for the four main meteorological seasons in Ireland, namely Spring (March, April, May), Summer (June, July, August), Autumn (September, October, November), and Winter (December, January, February). O_3 exceedances were calculated based on the WHO AQGs, indicating that the maximum daily average over eight hours (MDA8) should not exceed 100 µg/m³. A significant analysis was performed on data measured at the Mace Head Atmospheric Research Station (53°33′N, 9°54′ W), which is exposed to pristine marine air masses approximately half of the time. (Grigas et al., 2017; O'Dowd et al., 2014).

Table 1. Details of Environmental Protection Agency Ireland (EPA) O_3 measurement sites over Ireland, with location information, and the data period used for the study.

Site	Data availability	Type	Latitude	Longitude
Mace head	1994-2022	Coastal	53.3253	-9.9036
Valentia	2001-2022	Coastal	51.9385	-10.24
Monaghan	1995-2022	Rural	54.0661	-6.883
Laois	2005-2022	Rural	53.1076	-7.1983
Kilkenny	2012-2022	Rural	52.6383	-7.2676
Castlebar	2009-2022	Rural	53.851	-9.3003
Rathmines	2002-2022	Urban	53.322	-6.2672
Clonskeagh	2008-2022	Urban	53.3118	-6.2353
Swords	2009-2022	Urban	53.4631	-6.2222
Wicklow Bray	2009-2022	Urban	53.1873	-6.122
Cork South link road	2014-2022	Urban	51.8785	-8.4649
Cork Bishops town	2016-2022	Urban	51.8858	-8.53321
Cork UCC	2018-2022	Urban	51.9	-8.4863

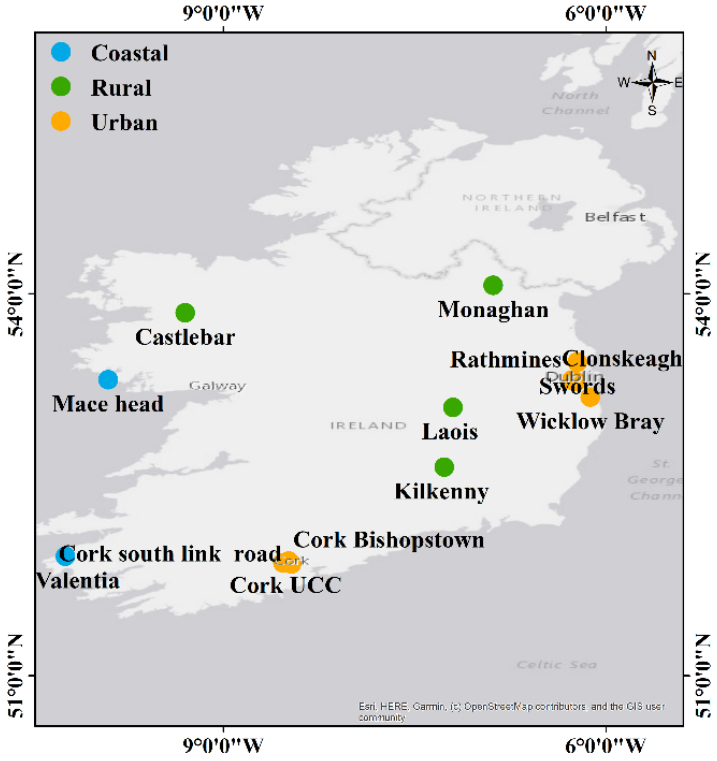

Figure 1. – The map of EPA O_3 measurement sites over Ireland with classification of backgrounds.

Trend analysis was conducted using the Openair package in R, software designed for the analysis of atmospheric composition data. Trends were determined using the Theil-Sen slope estimator and Mann-Kendall tests to quantify significance, in accordance with the Tropospheric Ozone Assessment Report (TOAR) guidelines (Lefohn et al., 2018). Theil-Sen directly provides a robust slope estimate. It is a reliable measure of change over time for direct interpretation and comparison. It is a robust method for estimating trend slopes in time series data, preferable to traditional least-squares regression, which can be sensitive to extreme values and outliers. Uncertainty or reliability of the trend is calibrated according to the p-value, as outlined by (Chang et al., 2023), consistent with the best statistical practices for analysis used in the second phase of TOAR.

2.2 Clean air sector identification from Back trajectories

Baseline O_3 refers to the concentration of O_3 in air masses minimally influenced by local or regional anthropogenic emissions. Back-trajectory methods are widely used to estimate baseline O_3 levels by analysing the origins and transport pathways of air masses reaching observation sites. Lagrangian dispersion models are used to trace air parcels backwards in time and identify their origin.

For this study, air mass trajectories arriving at Mace Head were calculated using the Hybrid Single Particle Lagrangian Integrated Trajectory Model (HYSPLIT) (Draxler et al.,2003; Stein et al., 2015) in conjunction with R software. The air masses were classified into two categories: the clean sector and EU-influenced sector. An air mass was considered part of the clean sector when air mass trajectories remained over the ocean surface for the previous 72 hours, the remaining air mass trajectories are classified as the EU-influenced sector. Meteorological data

for the analysis were derived from NOAA reanalysis data (Stunder et al., 2004). The 72h duration captures regional/long-range transport without trajectory error from meteorological uncertainties. The 100 m height was used to represent the well-mixed flow of the boundary layer above the surface. The 06:00 UTC aligns with synoptic times and can match daily O_3 cycles or measurement periods. Therefore, calculations were performed for 6:00 UTC each day, with a final trajectory height of 100 meters, covering the years 2000 to 2022. The O_3 concentrations observed during the clean sector were averaged to derive baseline levels, consistent with previous studies on baseline O_3 trends and sources (Derwent et al., 2013; Oltmans et al., 2006).

2.3 CAM4-Chem Model

The CAM-Chem air quality model, part of the Community Earth System Model (CESM), simulates atmospheric chemistry and the interactions among chemical constituents, meteorology, and climate. It incorporates detailed chemical mechanisms, emission inventories, and meteorological data to simulate pollutant dispersion, thereby allowing us to determine air quality trends. CAM-Chem has been applied in numerous studies, significantly contributing to the understanding of regional and global atmospheric processes. (Lamarque et al., 2012; Tilmes et al., 2016). The model features a flexible chemical pre-processor to allow for detailed handling of atmospheric chemistry. Studies have demonstrated that CAM-Chem accurately represents conditions in both the troposphere. (Aghedo et al., 2011; Lamarque et al., 2010) and the stratosphere (Lamarque et al., 2008; Lamarque and Solomon, 2010), including temperature structure and dynamics (Butchart et al., 2011). Offline CAM-Chem has also been utilised in the Hemispheric Transport of Air Pollution (HTAP) assessments. (Anenberg et al., 2009; Fiore et al., 2009; Jonson et al., 2010; Shindell et al., 2008;Tan et al., 2018).

For the current study, we analyse simulations of the Community Atmospheric Model version 4 CAM4-Chem (Community Atmosphere Model version 4 with chemistry) (Lamarque et al., 2012). The model simulations were carried out at a horizontal resolution of 210 km × 280 km, with 56 vertical levels for the 2000-2018 period, with specified dynamics derived from MERRA2 reanalysis. (Molod et al., 2015). The coarse spatial resolution, it is still appropriate because it provides a reliable representation of the regional background atmosphere influencing the urban sites. The model captures large-scale features of atmospheric transport, seasonal variability, and background O_3 levels, all of which are essential for interpreting urban observations. Comparing urban measurements with regional-scale CAM-Chem outputs allows local pollution effects to be distinguished from regional atmospheric influences.

Tagged source attribution of tropospheric ozone (TOAST 1.0) is a novel tagging methodology developed for the CESM to quantify source contributions to O_3. Unlike traditional methods that rely on sensitivity simulations, TOAST uses an online tagging approach to track O_3 production from specific NO_x and VOC sources (e.g., anthropogenic, biogenic, biomass burning, lightning) directly within the model, allowing for efficient attribution of O_3 to regional and sectoral emissions while maintaining full chemical coupling. The tool has been validated against observations and demonstrates utility in disentangling the impacts of different emission sectors on O_3 pollution. (Butler et al., 2018, 2020; Lupaşcu et al., 2022; Nalam et al., 2025). The model results have inherent standard uncertainties common in any modelling exercise, i.e., uncertainties in emission inventories in terms of magnitude and spatial accuracy; uncertainties in model parameters, e.g., surface resistance for deposition for various surfaces, boundary layer mixing, photolysis, chemical kinetic parameters (Wild et al., 2025) and structural deficiencies such as a coarse resolution and missing processes (e.g., halogen chemistry; Saiz-Lopez et al., 2025). The sum of all tagged contributions very closely matches the total simulated ozone

(which is simulated independently and is not just an algebraic sum of the tagged contributions) is a good validation of the tagging mechanism (Butler et al., 2018 and 2020).

Global CAM4-Chem model simulations are performed for the years 2000-2018 with NO_x and VOC tagging (as described in Ansari et al., 2025; Nalam et al., 2025), with the base chemical mechanism (Emmons et al., 2012) and source code modified to account for extra tagged species representing regional and sectoral identities. Anthropogenic emissions of NO_x, CO, and non-methane volatile organic compounds (NMVOCs) are incorporated from the Hemispheric Transport of Air Pollution version 3 emissions inventory. (HTAPv3; Crippa et al., 2024), which includes land-based emissions, international shipping emissions, and aircraft emissions. Biomass burning emissions are sourced from the GFED-v4 inventory (Van Der Werf et al., 2010), while biogenic NMVOC emissions are derived from CAM4-GLOB-BIO-v3.0. The O_3 source attribution technique used for this study is described in (Butler et al., 2020).

3. Results and discussions

3.1 Yearly variation of O_3

Figure 2 shows box plots, illustrating the average O_3 concentrations for 13 sites over the duration of the available dataset, as discussed in section 2.1 providing a comprehensive overview of the variability and distribution of O_3 concentration. Coastal sites, Mace Head and Valentia, show higher O_3 levels compared to other sites, with annual average concentrations of 77 µg/m³ and 69 µg/m³, respectively. In urban areas like Rathmines, Dublin, O_3 concentrations remained consistently lower, with averages ranging from 39 to 56 µg/m³. Similarly, South link road and Bishopstown sites in Cork city, recorded relatively lower concentrations compared to coastal and rural locations, reflecting the impact of high urban NO_x emissions. Rural sites like Laois and Kilkenny showed intermediate O_3 concentrations, less influenced by urban

emissions. These sites consistently show O_3 averages ranging between 50 to 57 µg/m³, with little variability, highlighting the predominant role of steady background O_3 contributions in rural sites. O_3 concentrations vary significantly with proximity to emission sources adjacent to urban areas. O_3 levels can be lower due to titration, where O_3 reacts with NO, causing O_3 depletion, but the transport of precursors can cause an increase in O_3 concentration downwind of the sources. (Jeon et al., 2014; Monks et al., 2015; Zhu et al., 2012)

The red line over the box shows a clear seasonal pattern in O_3 concentration for each site. With a springtime (March-April) peak and summertime (June-July), dip, with the highest peaks in the coastal sites, and lowest dips in urban sites, influenced by local emissions e.g. Cork South Link Road and Swords.

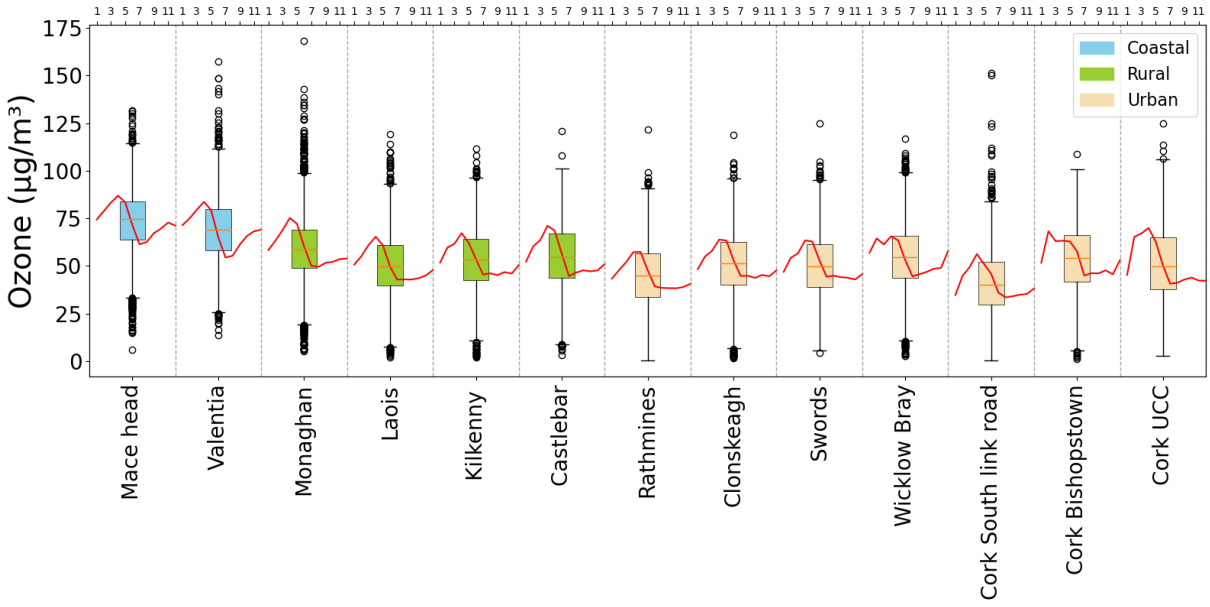

Figure 2. Annual average O_3 concentration at different sites in Ireland. In each box, the lowest whisker level represents the 5th percentile, the box spans from the 25th to the 75th percentile, the horizontal line within the box represents the median 50th percentile, and the upper whisker represents the 95th percentile. The average of monthly O_3 values calculated for the entire period of each station, and the red line shows the average monthly O_3 variation of all sites top axis shows the month (1– 12).

3.2 O_3 Trend analysis

3.2.1 Yearly trend

Table 2 summarises the Theil-Sen trends in O_3 concentration (in µg/m³ per year) across 13 monitoring sites in Ireland over different periods: 5 years (2018-2022), 10 years (2013-2022), 15 years (2008-2022), and the available years of data for each site. In the coastal regions, Mace Head shows a consistent decrease in O_3 levels over the 5, 10, and 15-year periods, although the entire dataset exhibits a small rising trend 0.02 µg/m³ per year. These trends are mostly in agreement with previous studies, where there was a positive trend observed in background O_3 up to the mid-2000s, which stabilised and began to decline in the 2010s (Derwent et al., 2018). Valentia shows a long-term decreasing trend of -0.23 µg/m³ per year, consistent with the previous study by Tripathi et al. (2010).

In rural areas, Monaghan exhibits a declining trend in O_3 concentrations across all time periods, indicating an overall reduction. Laois shows an upward trend over the 10 and 15-year periods, though there is a slight decline in the most recent 5 years. Kilkenny presents slight negative trends over the 5 and 10-year periods (-0.29 and -0.01µg/m³ per year). Negative trends are observed in Castlebar-(0.71 and -0.05 µg/m³ per year).

The Dublin urban area sites (Rathmines, Clonskeagh, Swords) predominantly show increasing trends in O_3 levels, indicative of changes in urban pollution or local emissions, with decreased suppression of O_3 levels in urban regions due to decreased local emissions. (Derwent et al., 2024). This is consistent with the "weekend effect," as observed by Atkinson-Palombo et al. (2006), whereby a reduction in NO_x due to reduced weekend traffic decreases O_3 removal by NO_x titration, leading to higher surface O_3 levels, likely to occur in wintertime, and in regions with low photochemical production due to low insolation and temperatures, as observed in

Ireland. It is duly noted that NO_x driven O_3 removal dominates over photochemical production in these sites. A comparable study in the UK carried out by Finch and Palmer (2020) attributed similarly rising trends in surface O_3 between 1999 and 2019 to decreasing NO_x, characterising UK observation sites as VOC-limited. Mixed results are observed at the urban stations of Cork, with a positive trend at the South-link Road and Bishopstown, but a negative trend at the UCC station. The UCC station, although classified as urban, lies within the university campus; hence, it would not be subject to significant local emissions. Coastal sites like Mace Head and Valentia generally show decreasing trends. These sites are less influenced by local emission sources, but with more significant impacts from regional and long-range transport, However, a detailed analysis of the trends requires consideration of seasonal effects.

Previous studies indicate that in northeast Europe, peak surface ozone concentrations have generally declined, reflecting the effectiveness of emission control measures (Yan et al., 2018). In contrast, background and lower-level O_3 concentrations have continued to increase, particularly at rural and suburban sites. Consistent with this, urban observations from 2000–2021 show increasing trends in median and lower-percentile O_3 levels, while the highest extremes have mostly decreased (Nelson et al., 2025).

Table 2. - Trends in surface O3 concentration (µg/m³ per year) calculated for 13 sites in Ireland over different periods over the complete dataset: 5 years (2018-2022), 10 years (2013-2022), 15 years (2008-2022), and the available measurement record for the site. The p-value evaluates the reliability of the trend, lower p-value indicating certainty. Adopting the trend reliability scale defined for TOAR-II studies (Chang et al., 2023), Statistical significance of trend is indicated using star notation: **** denotes $p \leq 0.01$ (very high certainty), *** denotes $0.01 < p \leq 0.05$ (high certainty), ** denotes $0.05 < p \leq 0.10$ (medium certainty), * denotes $0.10 < p \leq 0.33$ (low certainty), and no star denotes $p > 0.33$ (very low certainty).

Site No	Site name (Classification)	Measurement Record	Trend over record µg/m³ per year	5-year trend 2018-2022 µg/m³ per year	10-year trend 2013-2022 µg/m³ per year	15-year trend 2008-2022 µg/m³ per year
1	Mace Head (C)	1994-2022	0.02	-0.25	-0.31***	-0.11*
2	Valentia (C)	2001-2022	-0.23****	-1.15****	-0.84****	-0.32***
3	Monaghan (R)	1995-2022	-0.19****	-0.74**	-0.35**	-0.09*
4	Laois (R)	2005-2022	0.39****	-0.15	0.3**	0.46****
5	Kilkenny (R)	2012-2022	0.02	-0.29	-0.01	
6	Castlebar (R)	2009-2022	0.18**	-0.71**	-0.05	
7	Rathmines (U)	2002-2022	0.27****	1.72****	1.15****	0.48****
8	Clonskeagh (U)	2008-2022	0.33****	0.97***	0.12	0.33****
9	Swords (U)	2009-2022	0.6****	0.07	0.33****	
10	Wicklow Bray (U)	2009-2022	0.14*	0.04		
11	Cork Southlink Road (U)	2014-2022	0.51*	-0.44		
12	Cork Bishopstown (U)	2016-2022	1.05***	-1.81*		
13	Cork UCC (U)	2018-2022	-0.94	-0.94		

336

337 **3.2.2 Monthly trend**

338 Figure 3. shows the monthly trend for 10 years from the period 2012-2022. Mace Head
339 (coastal) and Monaghan (rural) sites predominantly show a rising trend in winter/early spring,
340 with a decreasing trend in late spring to summer. Valentia shows a decreasing trend in every
341 month except February when levels are significantly impacted by long-range transport and
342 stratospheric sources. (Auvray and Bey, 2005; Pan et al., 2018). Urban sites show a general
343 increasing monthly trend, but with a seasonal signal in Clonskeagh an increase in winter-spring
344 and a decrease in late spring or summer. Laois is characterised as a rural site yet exhibits rising
345 trends similar to the urban sites for all months except December, indicating that the

measurement station is affected by nearby emissions. Seasonal trends of the 15-year dataset are supplied in supplementary figure S2, where coastal stations exhibit a pronounced increase in late winter, and a decrease throughout the spring and summer, with a consistent near-year-round increase in Rathmines and Laois.

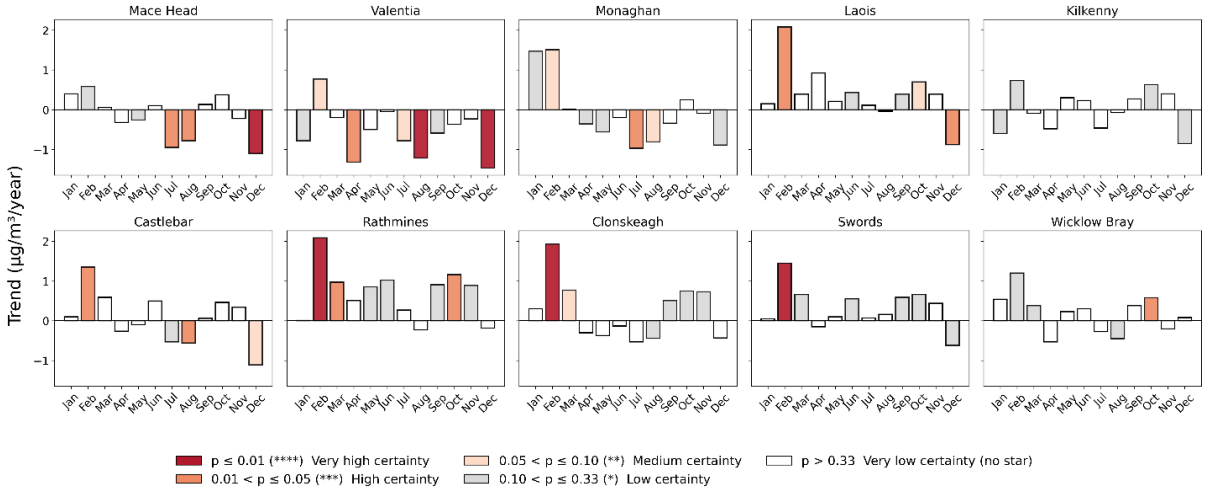

Figure 3. Monthly trend analysis of O_3 at different sites for 10 year period. (2012-2022) Adopting the trend reliability scale defined for TOAR-II studies (Chang et al., 2023), trends significance highlighted by colour.

3.3. O_3 Exceedance

The O_3 exceedances at 13 sites in Ireland over the available measurement dataset are identified according to WHO criteria, and the results are shown in Figure 4. The highest and lowest numbers of O_3 exceedances were observed at Mace Head and Rathmines, representing coastal and urban sites, respectively. Most exceedances occurred in spring (March, April, May), coinciding with the spring-time maximum. Rathmines had its highest number of exceedances in April 2019, while Laois reached a peak of 13 exceedances in May 2017. Castlebar and Swords show increased exceedance occurrences in spring and early summer, particularly notable spikes occurring in 2010, 2013, 2016, and 2019. Conversely, Wicklow Bray exhibited

a different pattern, showing significant spikes in February and March 2022, alongside occasional exceedances during March, April, and May, for example, in 2012 and 2018. Cork South link Road also recorded exceedances, particularly in March and notably in June. Cork Bishoptown shows exceedances, especially in February and March 2019, while Cork UCC recorded exceedances in April and May 2019. Kilkenny consistently exhibited exceedances during spring and summer, with April and May often recording the highest numbers, particularly in 2019. This highlights the impact of seasonal atmospheric conditions on O_3 levels. It is noted that summertime exceedances, although less frequent in occurrence, indicate photochemical production events that would be required to elevate O_3 levels from the annual dip in the seasonal cycle to exceed the WHO AQG threshold. These episodic spikes are characteristic of unique climatic or pollution events and warrant further study.

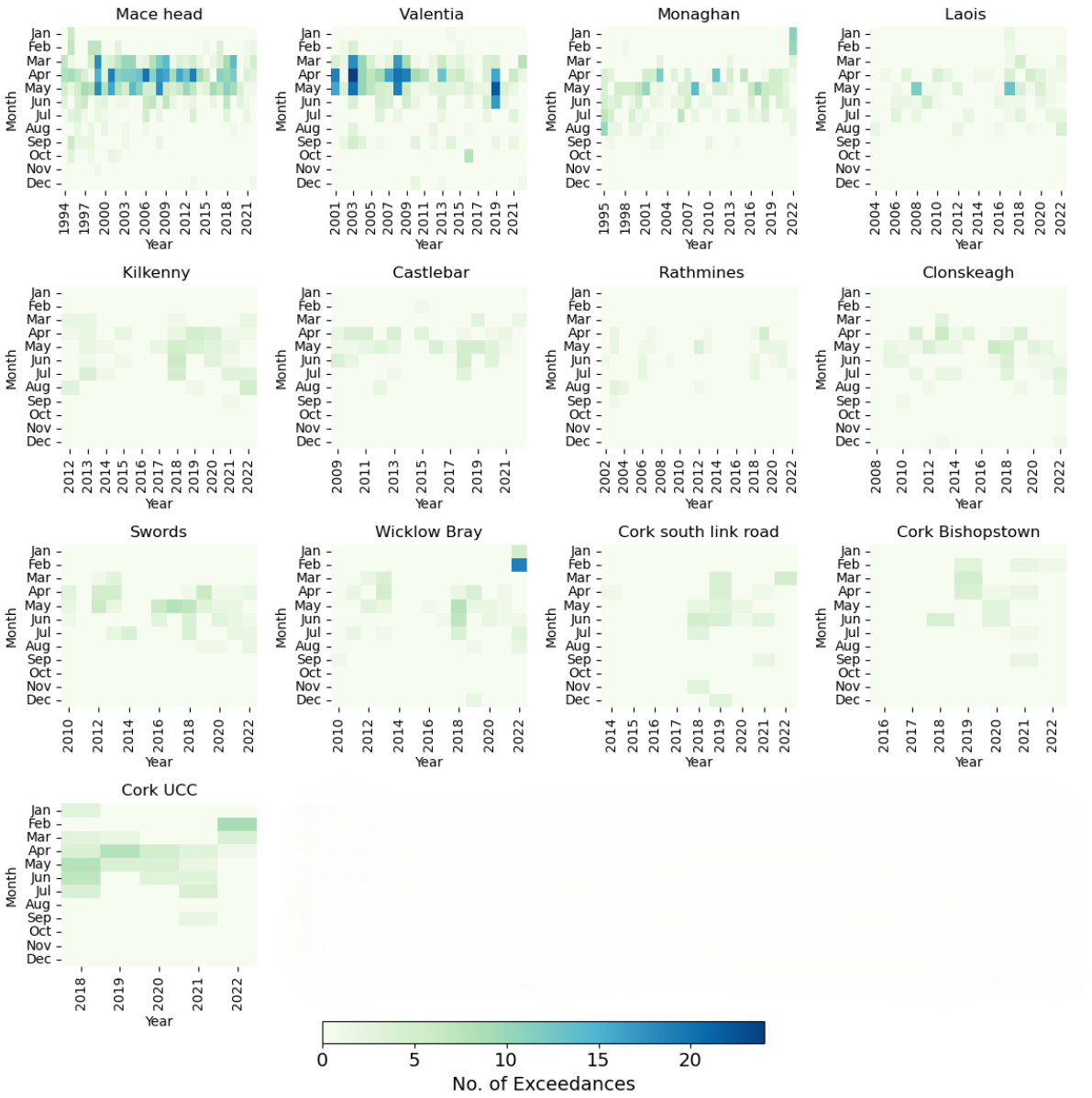

Figure 4. Monthly O_3 exceedances at different sites in Ireland. Exceedances are defined as days on which the maximum 8-hour running average of ozone (O_3) exceeds 100 µg/m³.

Figure 5 depicts trends in NO_2 and CH_4 concentrations across various Irish measurement sites. NO_2 trend calculations are based on site-specific data periods , Cork South link Road (2014–2022), Ballyfermot (2003–2022), Davit Road (2018–2023), Rathmines (1995–2024), Swords (2011–2025), Laois (2014–2026), Castlebar (2003–2027), Louth Dundalk (2019–2028), and Monaghan (2001–2029). For CH_4, the data cover the period 2010–2022. Most monitored sites exhibit a decreasing trend in NO_2 concentrations, most likely in response to pollution control

on transportation, industrial activities, and energy production in the EU and North America (Coleman et al., 2013; Donlon et al., 2024). In contrast, CH_4 levels observed at three sites Mace Head, Malin Head, and Carnsore Point indicate a significant and persistent rise in CH_4 concentrations. Mace Head is known for its clean Atlantic air and Malin Head, situated at Ireland's northern tip near the UK border, offers a unique position to observe both clean marine air and transboundary pollution, whereas Carnsore Point in the southeast, captures air masses from both the UK and mainland Europe (Spohn et al., 2022). These NO_2 and CH_4 trends reveal a dual dynamic: while NO_2 levels are decreasing due to effective emission controls, CH_4 levels relentlessly rise, highlighting the need for enhanced mitigation strategies targeting CH_4.

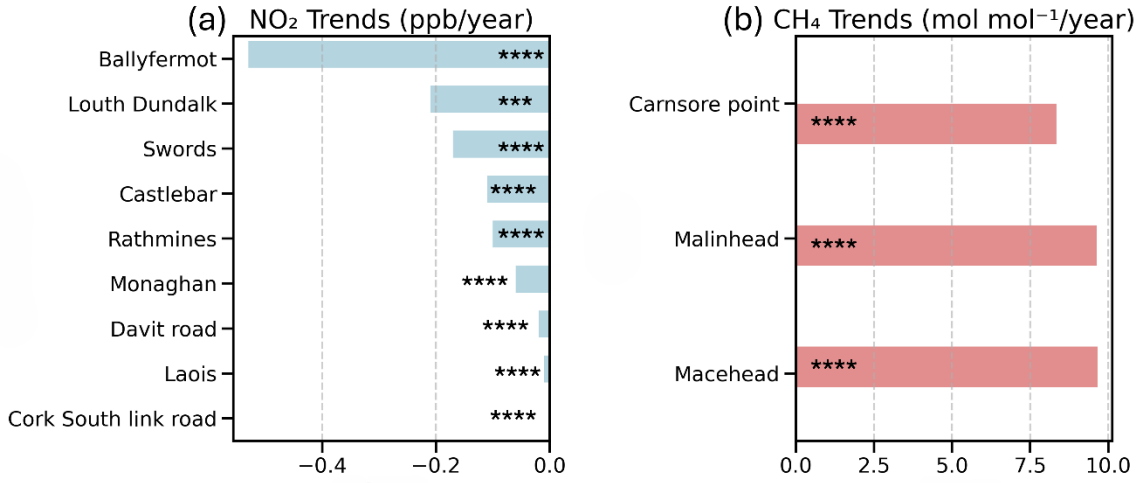

Figure 5. Trend in O_3 precursors NO_2 (a), and CH_4 (b) at different sites. Statistical significance of trend is indicated, increasing * with increasing trend reliability, as in Table 1.

To evaluate the relationship between NO_x and O_3 concentrations in an Irish context and the potential benefit of abrupt enforcement of NO_x control measures, we assess the impact of the COVID-19 2020 lockdown, Spring 2020, whereby the lockdown period saw a prominent relative decrease in NO_2, yet an increase in surface O_3 compared to average measurements for the same months 2017-2019 in most national monitoring stations (Figure 6). The negative

correlation between O_3 and NO_2 is indicative of a NO_x-saturated regime, normally associated with polluted urban environments and NO_x titration events. Analysis of the impact of the lockdown on Irish O_3 is discussed by Spohn et al. (2022), and a similar O_3 decrease was widely observed across Europe during the COVID lockdown (Ordóñez et al., 2020; Tavella & da Silva Júnior, 2021; C. Zhang & Stevenson, 2022). Significant enhancement of O_3 occurs at the inland measurement sites, despite a 2020 springtime decrease in O_3 observed at background coastal sites, Mace Head and Valentia. These coastal stations are less sensitive to changes in European NO_x emissions than inland sites and more sensitive to stratospheric and hemispheric transport (Tan et al., 2018). It is noted that April and May 2020 had unique meteorological conditions compared to previous years, with lower wind speed, less rain and significantly higher solar radiation, see Figure 12 in Spohn et al. (2022). These meteorological conditions would potentially facilitate photochemical O_3 production, contributing to positive O_3 anomalies during the lockdown period in addition to NO_x reduction, also potentially enhancing dry deposition to the ocean. Further investigation into this topic would warrant model sensitivity studies, beyond the scope of this current work.

The negative correlation between NO_x and O_3 under relatively clean atmospheric conditions indicates that O_3 levels are influenced predominantly by transport and chemical removal, and local photochemical production does not represent a significant surface O_3 source owing to periods of low-insolation periods and low temperature, which are characteristic of Irish meteorology and frequent cloud cover (Pallé and Butler, 2002).

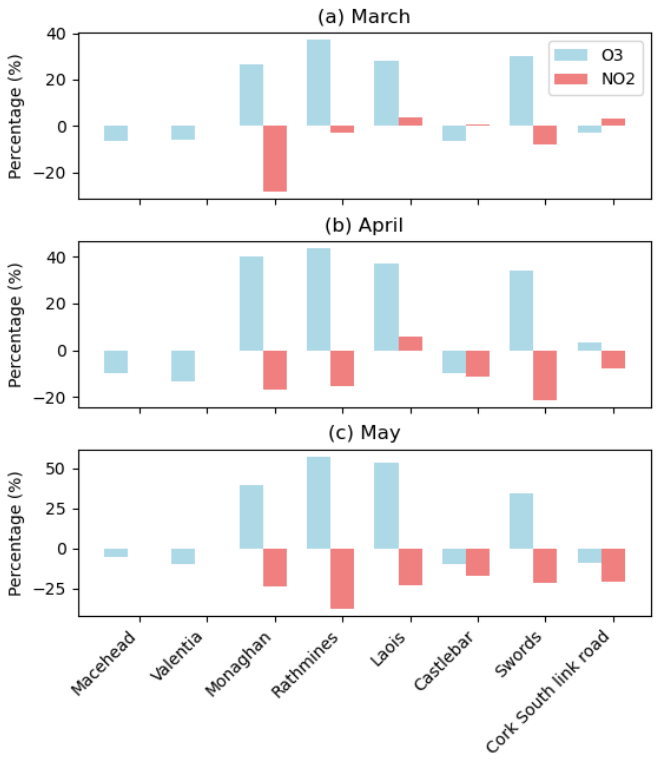

Figure 6. Percentage changes in NO_2 and O_3 during the lockdown period of 2020 as compared to the 2017-2019 average at different sites in Ireland for (a) March, (b) April, (c) May.

3.4 Model and Observations Comparison

3.4.1 Comparison between CAM4 – Chem Model and Observations

Global simulations were performed with the CAM4-Chem model enabled with source tagging (Butler et al., 2018) for 2000-2018, and the modelled O_3 over Ireland was compared with surface O_3 measurements at five sites. The grid details are shown in Figure S5. This model has already been comprehensively evaluated on a global scale (Nalam et al., 2025) against the TOAR-1 dataset, whereby the model performed well, albeit with a high bias attributable to the model's coarse resolution and implications for the resolution of urban chemistry (Ansari et al., 2025). Figure 7 shows the comparison of monthly O_3 CAM4-Chem and ground station O_3 data. From this figure, it is observed that CAM4-Chem exhibits a negative (positive) bias in rural and coastal (urban) sites. The consistent negative bias at Mace Head can be explained by the

435 coarse grid resolution, wherein the grid cell is not representative of clean marine Mace Head
436 conditions.

437 The influence of coastal meteorology, which suppresses O_3 formation due to cooler
438 temperatures and persistent cloud cover (McVeigh et al., 2010), also leads to an
439 underestimation of O_3 (Yerramilli et al, 2012). The dry deposition rate over land would exceed
440 that over the ocean, leading to a lower simulated O_3 concentration for the grid cell which covers
441 both land and ocean surface. Dry deposition is enhanced by solar radiation (Coleman et
442 al.,2012; Coleman et al., 2013; Pio et al., 2000), hence model measurement discrepancy is at a
443 maximum in late summer months. As outlined by Fiore et al. (2009), models average the
444 landscape characteristics within a grid cell, which can enhance O_3 deposition and result in lower
445 simulated O_3 concentrations; hence, the discrepancy is more pronounced in the clean sector
446 data.

447 Overestimation of O_3 in Clonskeagh and Cork South link Road is likely due to coarse grid
448 handling of localised emissions and subsequent atmospheric chemistry.

449

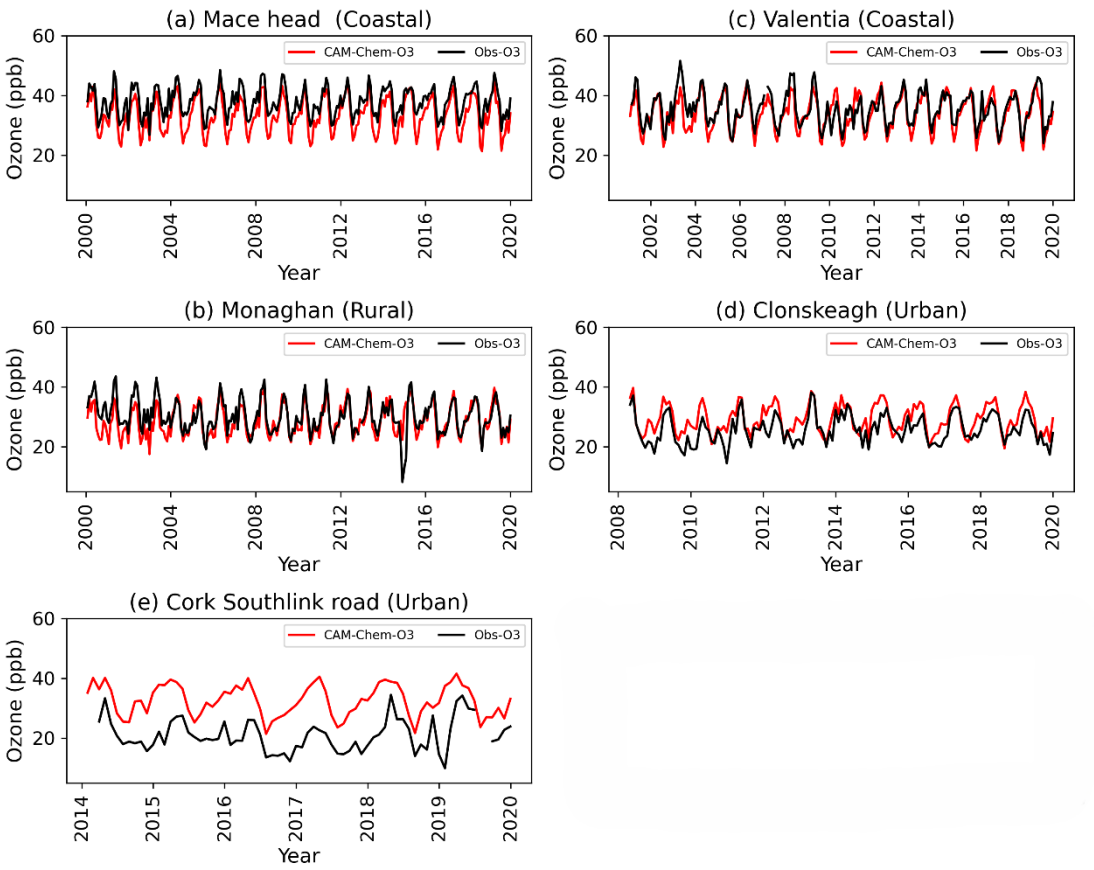

Figure 7. The comparison of Monthly CAM4 – Chem O_3 and Monthly O_3 observations at five sites in Ireland**.**

At Mace Head, the model shows a negative mean bias of - 4.42 (-11.68% normalized mean bias) but strong correlation (r =0.83). In Monaghan and Valentia, the model shows smaller biases of −1.43 and −1.54, normalized mean biases of −4.74% and −1.54%, and correlation coefficients of 0.73 and 0.72, respectively. These high correlations are in line with (Tilmes et al., 2015). However, at Clonskeagh and Cork South Link Road, the model overestimates, with positive biases (3.38 and 11.98) and weaker correlations (0.68 and 0.49). Statistics are given in the supplementary material, Table S1. These results suggest better model performance at coastal/rural sites and greater discrepancies in areas affected by local sources, as expected at this model resolution.

3.4.2 Source attribution using CAM4-Chem

To quantify the contribution of various precursor emission sources to modelled O_3 concentrations, the TOAST1.0 dual NO_x and VOC tagging technique was utilised (Butler et al., 2018). This allows attribution of modelled O_3 to the emissions of NO_x and VOC precursors across different source sectors and geographical regions as listed in Table 3.

Table 3. - List of tags used in NO_x and VOC tagging.

Regional Land-Based Tags		**Regional Oceanic Tags**		**Global Sector/Process-Based Tags**	
ARC	Arctic	**NAL**	North Atlantic	**AIR**	Aircraft
CAS	Central Asia	**ENA**	Eastern North Atlantic	**BIO**	Biogenic
EAS	East Asia	**NAE**	North America East Coast	**BMB**	Biomass Burning
EUR	Europe	**NAW**	North American West Coast	**LGT**	Lightning
MCA	Mexico & Central America	**NPA**	North Pacific	**STR**	Stratospheric Intrusion
MDE	Middle East	**BNS**	Baltic and North Seas	**XTR**	Extra untagged O_3
NAF	North Africa	**HBY**	Hudson Bay	**CH4**	Methane
NAM	North America	**IDO**	Indian Ocean	**OCN**	Oceanic Sources (DMS)
RBU	Russia-Belarus-Ukraine	**MBC**	Mediterranean, Black, and Caspian Seas	**SHP**	Shipping
SAS	South Asia	**SHO**	Southern hemispheric oceans	**AIR**	Aircraft
SEA	Southeast Asia			**INI**	Initial Condition O_3
VRW	Rest of the World				

The monthly tagged major precursor contributions to surface O_3 at Mace Head, averaged over the 2000-2018 simulation period, are shown in Figure 8. The stratospheric source of O_3 dominates in Winter-Spring, contributing to the spring-time maxima due to vigorous stratospheric transport. European NO_x emissions contribution peaks in May, while lightning NO_x has the greatest impact in winter. North American (NAM) NO_x emissions contribute 3.5 to 5.25 ppb, comparable to European NO_x, but with an earlier peak in April. Aviation emissions contribute 1 to 3 ppb, with the highest contributions in winter and spring. Biogenic NO_x, significant between June and October, contributes an average of 3.6 ppb, with higher contributions during August and September. O_3 derived from biogenic VOC sources average over 4 ppb during late autumn, maintaining a more sustained contribution throughout the year. East Asian NO_x emissions, contribute up to 3.6 ppb, with a minimum contribution in July and August. North Atlantic shipping NO_x (NAL) accounts for up to 2.4 ppb of O_3 during July. The total shipping NO_x (SHIP) also contributes significantly. It is the addition of all oceanic emissions and shows the highest contribution in June.

Methane (CH_4) is the dominant reactive carbon molecule contributing to O_3 formation. VOC emissions from biomass burning also play a measurable role, contributing 1 to 2 ppb, with their largest contributions in August and September. Finally, European VOC emissions contribute 1 to 3 ppb, with the largest impact from March to May, coinciding with the spring-time peak in surface O_3.

These findings allow quantification of specific sources amidst the complex interplay of regional and global sources in driving seasonal variations in surface O_3 levels over the Irish domain, highlighting the roles of stratospheric processes, anthropogenic emissions, biogenic sources, and lower-latitude contributions in shaping the observed patterns at background monitoring sites such as Mace Head.

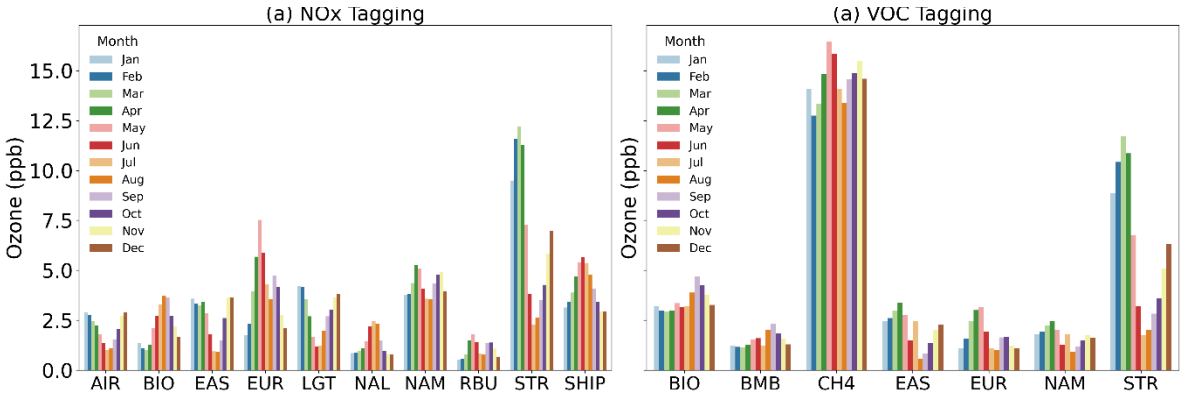

Figure 8. Absolute contribution of major NO_x sources (a) (NO_x Tagging) and VOC source (b) (NO_x Tagging) to the CAM4-Chem simulated surface O_3 for the Mace Head grid cell between 2000-2018.

Figure 9 shows the monthly changes in contributions to surface O_3 at Mace Head over the simulation period (2000-2018). A negative (blue) trend indicates that the contribution of the source to simulated surface O_3 in this grid cell has declined over the simulation period, whereas a positive trend (red) indicates the contribution to surface O_3 has risen. Figure 9 (a) shows that simulated O_3 at Mace Head originating from European or North American NO_x decreases over the simulation period, consistent with EU & NAM emission reductions. (Guerreiro et al., 2014). More significant reduction occurs in late Spring through late summer, when EU NO_x contributions are most significant to Mace Head O_3 concentrations (as seen in Figure 8).

There is a rising trend in simulated surface O_3 originating from NO_x emissions from global aviation, from East Asia, and to a lesser extent from South Asia, which is more pronounced in the wintertime. Wintertime temperatures in South Asia are still high enough to sufficiently produce local ozone, especially when NOx emissions are rising (Crippa et al., 2023). The relatively longer atmospheric lifetime of O_3 in the free troposphere during winter enables longer-range intercontinental transport (Huang et al., 2017;Yu et al., 2013). This seasonality

in source contributions explains the observed reduction in spring-time maxima and increase in winter-time levels from the measurement record. East-Asian and South-Asian VOCs also contribute to a rising trend in simulated O_3, with a more pronounced increase in winter and spring. This highlights a different pattern in hemispheric O_3 contributions, where EU and NAM emission reductions coincide with increased contribution from lower latitudes, which could potentially become a more significant source of background O_3 in the Northern Hemisphere in the future. The contribution of CH_4 also has a positive trend over the simulation period, but the CH_4 trend has a reliable correlation only in December and spring periods, with very low certainty in CH_4 contribution trends for summer months (correlation coefficient, $p>0.33$). Contribution to simulated O_3 at Mace Head from EU and NAM anthropogenic VOC show a negative trend for all months, consistent with trends from EU and NAM anthropogenic NO_x.

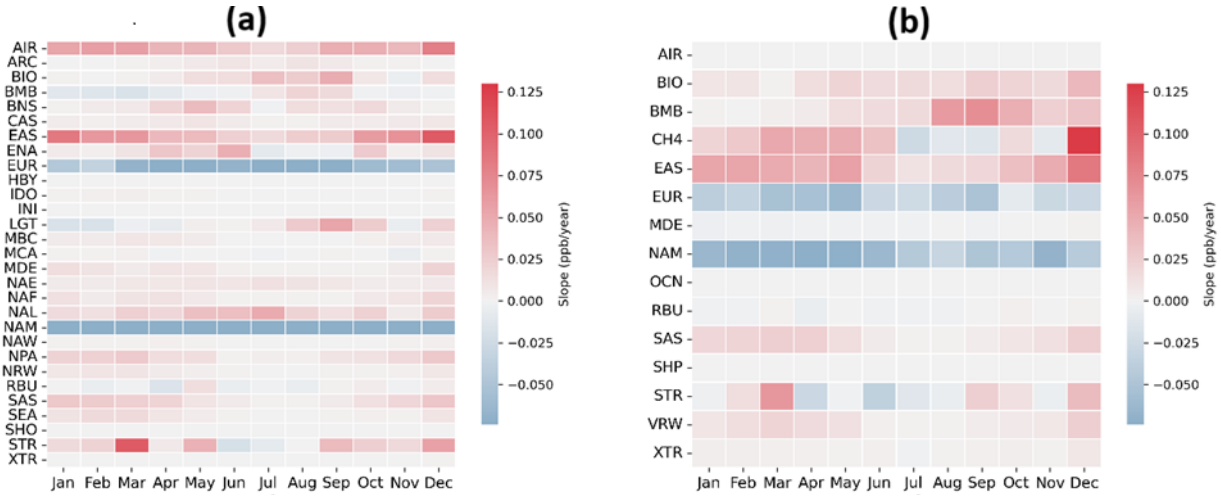

Figure 9. Trends in contributions to the monthly average modelled Mace Head grid cell surface O_3 at for the 2000-2018 period derived from (a) NO_x tagging and (b)VOC tagging.

Table 4. shows the overall trend in the main contributors to NO_x and VOC tagging. It is observed that there is an increase in simulated surface O_3 originating from NO_x contributions from aviation and East Asia, while there is a decrease in European (EUR) and North American (NAM) NO_x contributions. In VOC tagging, Methane (CH_4) and East Asian anthropogenic

VOC (EAS) contribute to a rising trend over the simulation period, whereas anthropogenic VOC contributions from Europe (EUR) and North America (NAM) show a negative trend.

Table 4 - Overall Trend in contributions to Mace Head grid cell O_3 simulated by CAM4-Chem for NO_x tagging and VOC tagging over the simulation period in units of ppb per year. reliability scale defined for TOAR-II studies (Chang et al., 2023), Statistical significance of trend is indicated using star notation: **** denotes $p \leq 0.01$ (very high certainty), *** denotes $0.01 < p \leq 0.05$ (high certainty), ** denotes $0.05 < p \leq 0.10$ (medium certainty), * denotes $0.10 < p \leq 0.33$ (low certainty), and no star denotes $p > 0.33$ (very low certainty).

NO_x Tagging		**VOC Tagging**	
	Slope (ppb/year)		Slope (ppb/year)
AIR	0.0467****	CH_4	0.0590****
EAS	0.0491****	EAS	0.0333****
EUR	-0.0900****	EUR	-0.0553****
NAM	-0.1243****	NAM	-0.0670****

3.5 O_3 Trends in Background and EU influenced sector Airmasses at Mace Head

Although Mace Head is classified as a global background site, quantification of the baseline pollution levels requires trajectory analysis, whereby both measured and modelled data is filtered to limit the data to that arriving from the clean sector, unaffected by land-based emission sources, as discussed in Section 2.2. Figure 10 displays trends in observed and simulated O_3 at Mace Head, separated into seasons and clean/EU influenced sectors according to the trajectory analysis. The figure shows that the clean sector has consistently higher O_3 concentrations than the EU influenced sector for Winter, Spring and Autumn, with the most significant disparity between clean and EU sectors in winter/spring when stratospheric intrusion and lightning NO_x contribute most significantly to O_3, as discussed in Section 3.4.2. O_3 originating from EU airmasses is susceptible to higher rates of dry deposition and removal

via local pollution while traversing the land-mass westwards towards Mace Head, leading to higher O_3 in clean-sector air masses consistent with previous studies (Coleman et al., 2013). A decreasing trend in mean spring-time levels is observed for both clean and EU influenced sectors, consistent with the sustained decrease in precursor emissions in Europe and North America as displayed in Figure 9. An increasing trend (0.26 ppb/year) is observed in the winter-time EU influenced sector, with a trend of smaller magnitude (0.08 ppb/year) observed in the clean sector, indicating a decrease in winter-time O_3 depletion events due to decreasing European emissions (from the EU influenced sector), consistent with the conclusions from previous studies of Mace Head surface O_3 (Derwent et al., 2024). Summer-time values do not exhibit a notable trend or a discrepancy between the clean and EU influenced sector measurements, indicating that there is little O_3 advected into Europe from the west in the summer months. It is noted that the seasonal trends exhibit slopes with p-values ranging between $0.1 > p > 0.01$, which denote trends of medium to high certainty, as defined by TOAR assessment criteria of Chang et al., 2023.

Although the model results display a negative bias for reasons outlined in section 3.4.1, the clean sector consistently exhibits higher simulated O_3 concentrations than the EU-influenced sector, except during the summer season. In the winter season, a significant increasing trend is observed for simulated O_3 from both sectors, aligning with observations. A decreasing trend is observed during the summer season, again consistent with the observations for both sectors. In spring and autumn, modelled O_3 exhibits a positive trend over the simulation period.

Trends in contributors of model O_3 during the different seasons for the clean and EU-influenced sector are shown in Tables S3 to S4 in the supplementary material. Aviation and East Asian NO_x show consistently positive and significant trends in both sectors, while North America NO_x shows strong negative trends throughout the year in the clean sector. For the EU-influenced sector in NO_x tagged (Table S2), similar positive trends observed for aviation and

East Asian, with North America NO_x remaining negative and European NO_x showing more significant declines in spring and winter. In case of VOC tagged O_3, the East Asian VOCs shows an increasing trend and North America VOCs show a negative across all seasons in both sectors (Table S3 and S4). European VOCs also show a consistent negative trend, particularly strong in the EU-influenced sector. Methane trends are seasonally positive, especially in spring and winter.

It is observed that the model consistently simulates O_3 at lower concentrations than that observed at Mace Head. This is not surprising, considering the coarse resolution of the model, which limits its ability to represent fine-scale processes and dry deposition accurately. Dry deposition is typically higher over land, and the grid cell covering Mace Head includes land area, as shown in Figure S5 of the supplementary material. Further, as explained by Fiore et al. (2009), models average the landscape characteristics within a grid cell, which can enhance O3 deposition and result in lower simulated O_3 concentrations; hence, the discrepancy is more pronounced in the clean sector data.

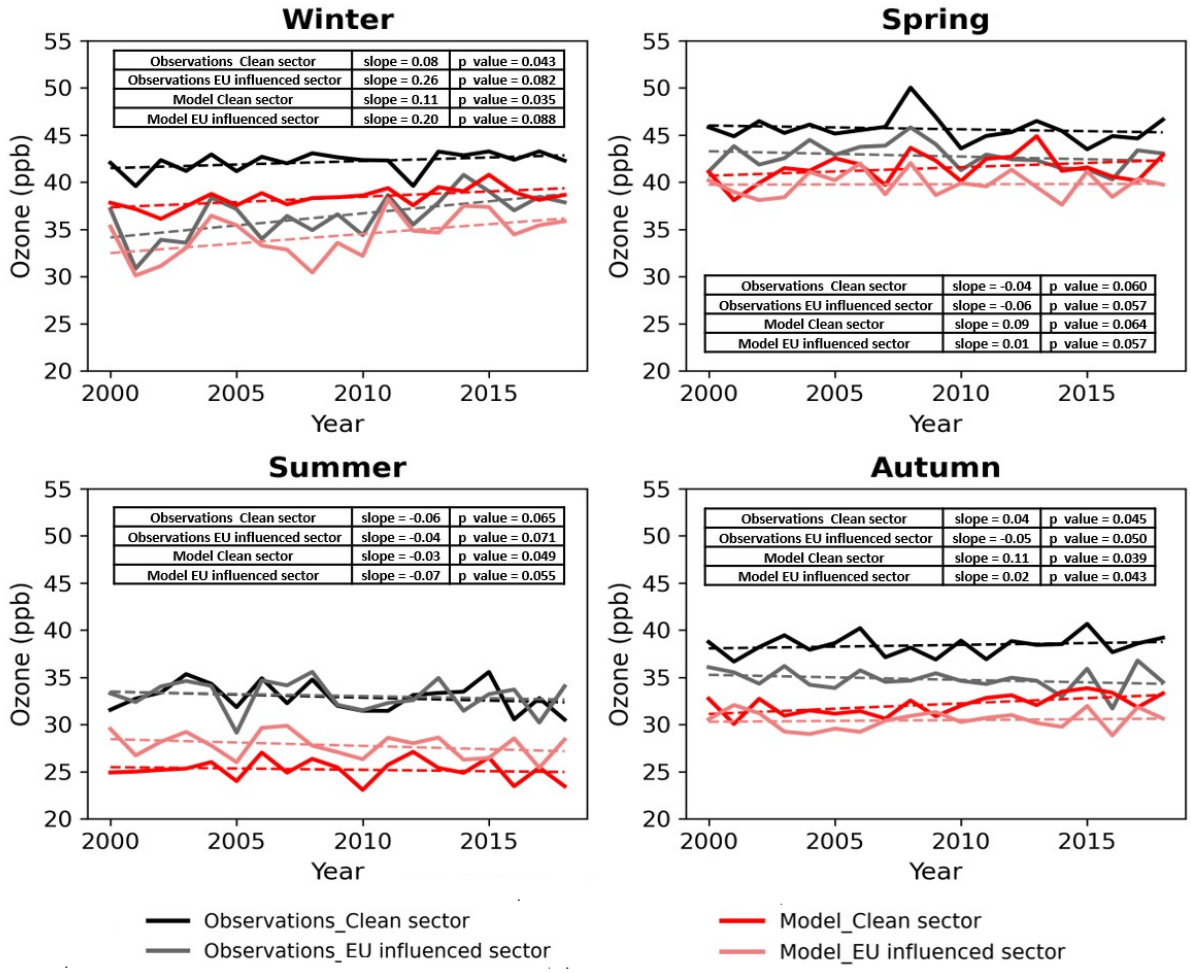

Figure 10. - Trend in seasonal Average of observed O_3 (black) and Model O_3 (red) at Mace Head, separated into clean sector and EU-influenced sector.

3.6 Exceedances from the clean and EU-influenced sector at Mace Head

Exceedances observed at Mace Head between 2000 and 2022 are separated into clean and EU-influenced sectors based on trajectory air masses and shown in Figure 11. 35% of all exceedances for this period occurred in clean air masses, the remainder occurring when air masses include EU outflow and contribution from local sources to enhance surface O_3 at Mace Head, which is already elevated compared to inland and urban sites. It is notable that there is a higher proportion of exceedances that occur from EU- influenced sector, despite higher mean observations from the clean sector for all seasons This occurs because of an enhancement of surface O_3 occur during an influx of polluted air from the EU, UK or local sources. The EU

influence on exceedance becomes more proportionally prominent in late Spring and summer, with more frequent easterly airflow when there is a higher occurrence of stagnation events.

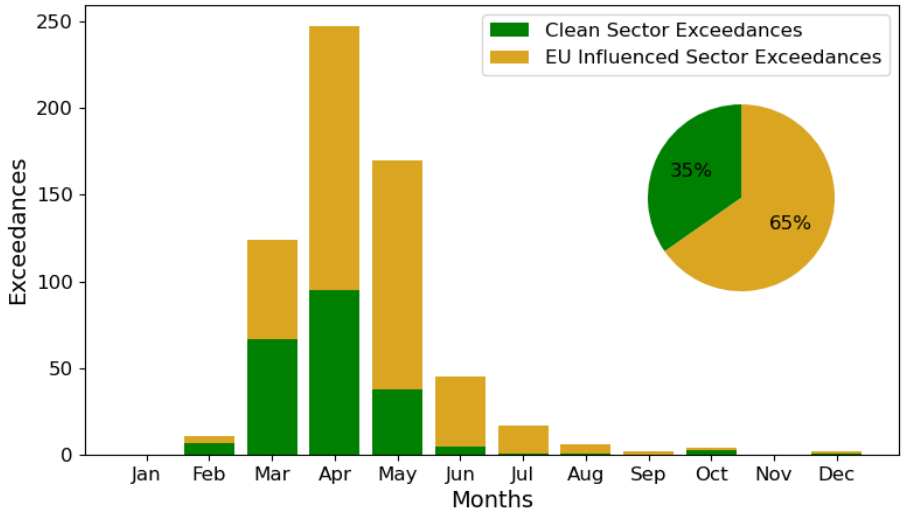

Figure 11. Exceedances measured at Mace Head per month from 2000 until 2022, during the clean air sector(green) and EU influenced sector (yellow). The percentage of both to total exceedances is shown in the inlay.

Figure 12 shows the trend in spring-time exceedances and the 95th percentile Springtime O_3 measured at Mace Head between 2000 and 2022. A decreasing trend in exceedances is observed, with a greater decreasing trend in from the EU and locally influenced sector. This indicates that the changes that are driving the reduction in the exceedances in Europe are coming into effect at a quicker rate than the changes that are driving the O_3 event reduction over the North Atlantic. The trends in the exceedance counts are not significant, according to the criteria in Chang et al., 2023, but there is a statistically significant decreasing trend in the 95th percentile springtime surface O_3 over the measurement record. Figure 12 (b) shows the trend in spring-time surface O_3 measured at Mace Head segregated into Clean and EU-influenced sector. The trend is more significant both in magnitude and statistical certainty for the EU-influenced sector, indicating that European emission changes have a more pronounced

effect on springtime O_3 measured at Mace Head O_3 as compared to changes affecting O_3 transported or formed over the North Atlantic.

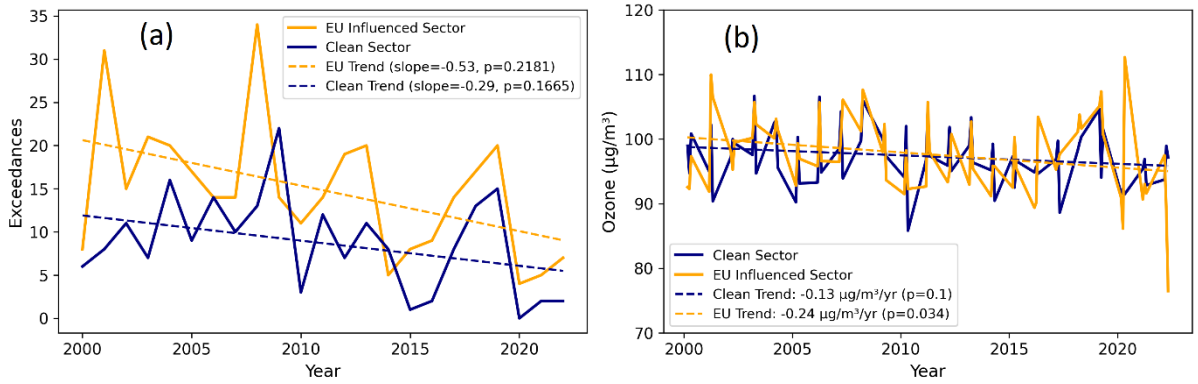

Figure 12. (a) The trend in Spring-time exceedances measured at Mace Head between 2000 and 2022 (blue) with the clean-air exceedances (gold), and (b) The trend in 95$^{th\ percentile}$ of spring (Mar- May) O_3 measured in mg /m^3 for the clean sector (blue) and the EU-influenced sector (gold).

Figure 13 shows monthly cumulative contributions to simulated O_3 concentrations within the Mace Head grid cell for NO_x and VOC tagging during O_3 exceedance. First, the exceedances were identified from O_3 observations as discussed in Section 3.3 and then these exceedances were divided into two sectors the EU-influenced sector and the clean sector. In Figure 13, the hourly O_3 exceedance cumulative concentrations in ppb, along with the contributions from different parameters, are shown. It indicates which parameters contribute more to the exceedances, in both the EU-influenced sector or the clean sector. In this the ug/m3 to ppb conversion is considered for the exceedances.

These exceedances are categorised into clean and EU-influenced sectors. The maximum exceedances are observed in March to May. From Figure 13 (a), it is clear that stratospheric intrusion, North American NO_x, European NO_x, and East Asian NO_x are the major contributors

637 driving exceedances at Mace Head during the spring months (March to May). European
638 emissions dominate the supply of NO_x precursors in April, reaching their peak in May. Figure
639 13 (b) shows that CH_4 is the most dominant VOC source, followed by stratospheric intrusion
640 and Biomass burning. North American and European VOC emissions also contribute
641 significantly to O_3 formation during this period. Collectively, these findings highlight the
642 complex interplay of regional and global sources in driving surface O_3 exceedances over the
643 Irish domain.

644 North American NO_x also contributes significantly to exceedance in both clean and EU-
645 influenced sectors at Mace Head during March to May month, likely due to long-range
646 transport and mixing, regional stagnation or synoptic-scale recirculation. In the case of VOC
647 tagging, stratospheric intrusion, and CH_4 show notable contributions. Biomass burning, East
648 Asian emissions and North American VOC emissions also play a role in O_3 exceedances. The
649 IN_SHIP indicates the total contribution of all international shipping emissions
650 (ENA,NAE,NAW,NPA,BNS,HBY,IDO,MBC,SHO) which is significant in April and May.

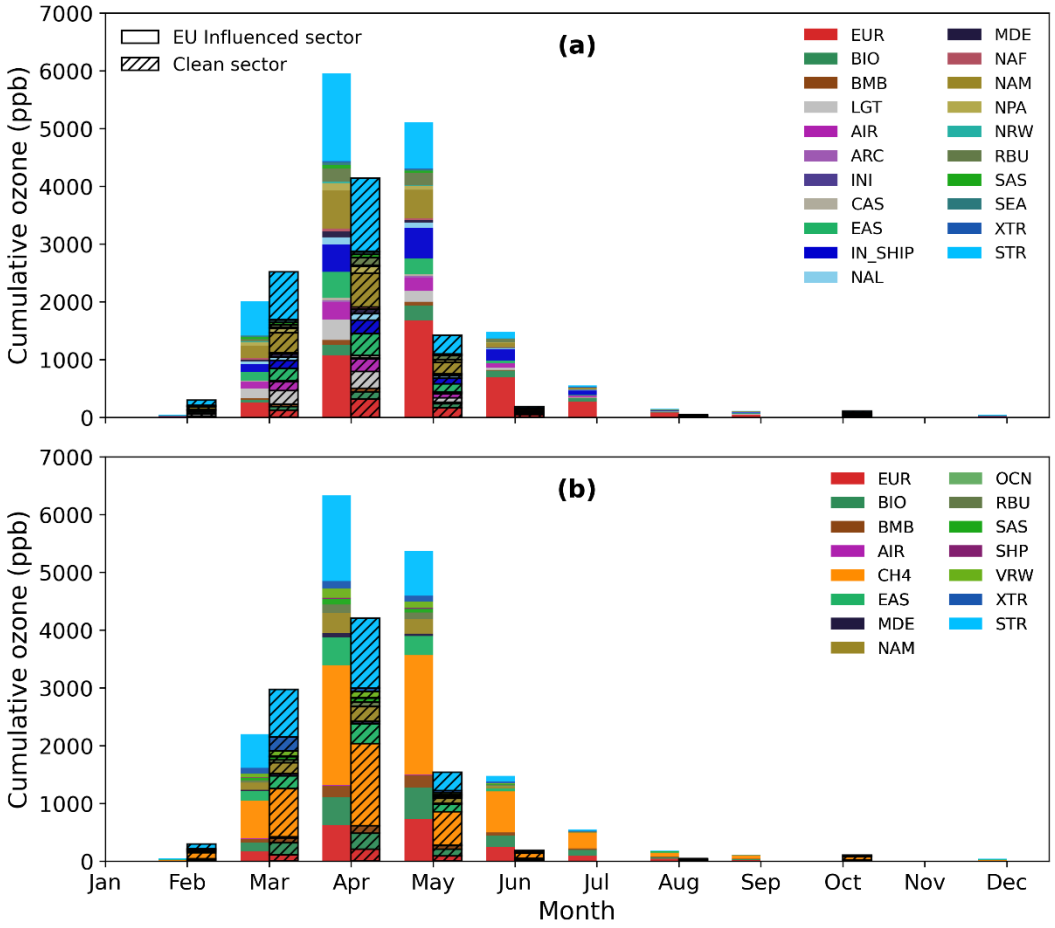

651

652 **Figure 13** - Monthly cumulative Mace Head grid cell O_3 contributions to EU influenced sector

653 and clean sector exceedances (a) NO_x tagging and (b) VOC tagging Mace Head grid cell.

654 **4. Conclusion**

655 This study highlights the complexities of O_3 pollution in Ireland, revealing that coastal areas

656 experience higher O_3 concentrations than rural and urban environments, attributed to the effect

657 of transboundary pollution and stratospheric intrusion. Over the last two decades, urban sites

658 have shown a significant increasing trend in O_3 levels, particularly in winter, influenced by

659 decreasing anthropogenic pollution in Europe, the UK, North America and local to the

660 observation sites, representing a decline in chemical removal mechanism (Derwent et al., 2024;

661 Simmonds and Derwent, 1991). The analysis also points out that the majority of exceedances

662 at coastal monitoring sites coincide with the annual spring maxima. Using the advanced

capabilities of the CAM4-Chem model with dual NO_x and VOC tagging, we identified key factors affecting seasonal O_3 variations, such as the spring-time peak and summer dip, driven by a mix of stratospheric intrusion, NO_x emissions from lightning, long range and hemispheric transport, regional emissions and aviation related emissions. Trend analysis from simulation results identified East Asian and aviation emissions as significant contributors to the rising winter trends in O_3, while reductions in North American and European emissions accounted for the decrease in spring peaks. This study provides a comprehensive understanding of the various factors affecting O_3 levels in Ireland, offering important insights for the development of O_3 pollution control policies.

Data availability

All data are available upon request.

Author contributions

LC designed the study. NK analysed the data and wrote the manuscript. TA and TB provided CAM-Chem model results and reviewed the manuscript. C.C. assisted with the interpretation of results and manuscript editing. EC. Assisted with the back trajectories analysis. DM contributed to the study design. JO, DC, and CD reviewed the manuscript and edited it.LC edited it with contributions from all coauthors.

Competing interests

The authors declare that at least one of the authors sits on the editorial board of ACP.

Acknowledgement - The authors acknowledge the Environmental Protection Agency (EPA) of Ireland for their financial support of the Ozone project under the EPA Research Programme 2021-2030 (project number 2022-CE-1133), and the European Union's Horizon Europe

686 Research and Innovation programme under HORIZON-CL5-2022-D1-02 (grant no.
687 101081430-PARIS).

688

689 **References**

690 Aghedo, A. M., Bowman, K. W., Worden, H. M., Kulawik, S. S., Shindell, D. T., Lamarque, J.
691 F., Faluvegi, G., Parrington, M., Jones, D. B. A., and Rast, S.: The vertical distribution of ozone
692 instantaneous radiative forcing from satellite and chemistry climate models, Journal of
693 Geophysical Research Atmospheres, 116, https://doi.org/10.1029/2010JD014243, 2011.

694 Anenberg, S. C., West, J. J., Fiore, A. M., Jaffe, D. A., Prather, M. J., Bergmann, D., Cuvelier,
695 K., Dentener, F. J., Duncan, B. N., Gauss, M., Hess, P., Jonson, J. E., Lupu, A., Mackenzie, I.
696 A., Marmer, E., Park, R. J., Sanderson, M. G., Schultz, M., Shindell, D. T., Szopa, S., Vivanco,
697 M. G., Wild, O., and Zeng, G.: Intercontinental impacts of ozone pollution on human mortality,
698 Environ Sci Technol, 43, 6482–6487, https://doi.org/10.1021/es900518z, 2009.

699 Ansari, T., Nalam, A., Lupaşcu, A., Hinz, C., Grasse, S., & Butler, T.: Explaining trends and
700 changing seasonal cycles of surface ozone in North America and Europe over the 2000–2018
701 period: a global modelling study with NOx and VOC tagging, Atmospheric Chemistry and
702 Physics, 25, 16833–16833. https://doi.org/10.5194/acp-25-16833-2025,2025.

703 Archibald, A. T., Neu, J. L., Elshorbany, Y. F., Cooper, O. R., Young, P. J., Frost, G. J., Galbally,
704 I. E., Gerosa, G., Granier, C., and Griffiths, P. T.: Tropospheric Ozone Assessment Report : A
705 critical review of changes in the tropospheric ozone burden and budget from 1850 to 2100, 1–
706 53, 2020.

707 Ashmore, M. R.: Assessing the future global impacts of ozone on vegetation, Plant Cell
708 Environ, 28, 949–964, https://doi.org/10.1111/j.1365-3040.2005.01341.x, 2005.

709 Atkinson-Palombo, C. M., Miller, J. A., and Balling, R. C.: Quantifying the ozone “weekend
710 effect” at various locations in Phoenix, Arizona, Atmos Environ, 40, 7644–7658,
711 https://doi.org/10.1016/j.atmosenv.2006.05.023, 2006.

712 Auvray, M. and Bey, I.: Long-range transport to Europe: Seasonal variations and implications
713 for the European ozone budget, J. Geophys. Res., 110, D11303,
714 https://doi.org/10.1029/2004JD005503, 2005.

715 Bessagnet, B., Pirovano, G., Mircea, M., Cuvelier, C., Aulinger, A., Calori, G., Ciarelli, G.,
716 Manders, A., Stern, R., Tsyro, S., Garciá Vivanco, M., Thunis, P., Pay, M. T., Colette, A.,
717 Couvidat, F., Meleux, F., Rouïl, L., Ung, A., Aksoyoglu, S., Baldasano, J. M., Bieser, J.,
718 Briganti, G., Cappelletti, A., D’Isidoro, M., Finardi, S., Kranenburg, R., Silibello, C.,
719 Carnevale, C., Aas, W., Dupont, J. C., Fagerli, H., Gonzalez, L., Menut, L., Prévôt, A. S. H.,
720 Roberts, P., and White, L.: Presentation of the EURODELTA III intercomparison exercise-
721 evaluation of the chemistry transport models’ performance on criteria pollutants and joint
722 analysis with meteorology, Atmos Chem Phys, 16, 12667–12701, https://doi.org/10.5194/acp-
723 16-12667-2016, 2016.

724 Bonaccorso, B., Peres, D. J., Cancelliere, A., and Di Mauro, G.: Probabilistic forecasting of
725 drought class transitions in Sicily (Italy) using Standardized Precipitation Index and North
726 Atlantic Oscillation Index, Hydrol. Earth Syst. Sci., 19, 389–404, 2015.

727 Boylan, P., Helmig, D., and Oltmans, S.: Ozone in the Atlantic Ocean marine boundary layer,
728 1–13, https://doi.org/10.12952/journal.elementa.000045, 2014.

729 Butchart, N., Charlton-Perez, A. J., Cionni, I., Hardiman, S. C., Haynes, P. H., Krüger, K.,
730 Kushner, P. J., Newman, P. A., Osprey, S. M., Perlwitz, J., Sigmond, M., Wang, L., Akiyoshi,
731 H., Austin, J., Bekki, S., Baumgaertner, A., Braesicke, P., Brhl, C., Chipperfield, M., Dameris,
732 M., Dhomse, S., Eyring, V., Garcia, R., Garny, H., Jöckel, P., Lamarque, J. F., Marchand, M.,

Michou, M., Morgenstern, O., Nakamura, T., Pawson, S., Plummer, D., Pyle, J., Rozanov, E., Scinocca, J., Shepherd, T. G., Shibata, K., Smale, D., Teyssèdre, H., Tian, W., Waugh, D., and Yamashita, Y.: Multimodel climate and variability of the stratosphere, Journal of Geophysical Research Atmospheres, 116, https://doi.org/10.1029/2010JD014995, 2011.

Butler, T., Lupascu, A., Coates, J., and Zhu, S.: TOAST 1.0: Tropospheric ozone attribution of sources with tagging for CESM 1.2.2, Geosci Model Dev, 11, 2825–2840, https://doi.org/10.5194/gmd-11-2825-2018, 2018.

Butler, T., Lupascu, A., and Nalam, A.: Attribution of ground-level ozone to anthropogenic and natural sources of nitrogen oxides and reactive carbon in a global chemical transport model, Atmos Chem Phys, 20, 10707–10731, https://doi.org/10.5194/acp-20-10707-2020, 2020.

Carslaw, D. C.: On the changing seasonal cycles and trends of ozone at Mace Head, Ireland, Atmos. Chem. Phys, 3441–3450 pp., 2005.

Chang, K.-L., Schultz, M. G., Koren, G., and Selke, N.: Guidance note on best statistical practices for TOAR analyses, 2023.

Coates, J., Mar, K. A., Ojha, N., & Butler, T. M.: The influence of temperature on ozone production under varying NO x conditions–a modelling study. Atmospheric Chemistry and Physics, 16(18), 11601-11615, 2016.

Coleman, L., McVeigh, P., Berresheim, H., Martino, M., and O'Dowd, C. D.: Photochemical impact on ozone fluxes in coastal waters, Advances in Meteorology, 2012, https://doi.org/10.1155/2012/943785, 2012.

Coleman, L., Martin, D., Varghese, S., Jennings, S. G., and O'Dowd, C. D.: Assessment of changing meteorology and emissions on air quality using a regional climate model: Impact on ozone, Atmos Environ, 69, 198–210, https://doi.org/10.1016/j.atmosenv.2012.11.048, 2013.

Creilson, J. K., Fishman, J., & Wozniak, A. E. Intercontinental transport of tropospheric ozone: A study of its seasonal variability across the North Atlantic utilizing tropospheric ozone residuals and its relationship to the North Atlantic Oscillation. Atmospheric Chemistry and Physics, 3(6), 2053–2066. https://doi.org/10.5194/acp-3-2053-2003,2003.

Crippa, M., Guizzardi, D., Butler, T. M., Keating, T., Wu, R., Kaminski, J., Kiesewetter, G., Im, U., Bessagnet, B., Chabrillat, S., et al.: The HTAP_v3 emission mosaic: merging regional and global monthly emissions (2000–2018) to support air quality modelling and policies, Earth Syst. Sci. Data, 15, 2667–2696, 2023.

Crippa, M., Guizzardi, D., Pagani, F., Schiavina, M., Melchiorri, M., Pisoni, E., Graziosi, F., Muntean, M., Maes, J., Dijkstra, L., Van Damme, M., Clarisse, L., and Coheur, P.: Insights into the spatial distribution of global, national, and subnational greenhouse gas emissions in the Emissions Database for Global Atmospheric Research (EDGAR v8.0), Earth Syst Sci Data, 16, 2811–2830, https://doi.org/10.5194/essd-16-2811-2024, 2024.

Derwent, R. G.: Observation and interpretation of the seasonal cycles in the surface concentrations of ozone and carbon monoxide at Mace Head, Ireland from 1990 to 1994, Atmos Environ, 32, 2310, https://doi.org/10.1016/S1352-2310(97)00338-5, 1998.

Derwent, R. G., Simmonds, P. G., and Collins, W. J.: Ozone and carbon monoxide measurements at a remote maritime location, mace head, Ireland, from 1990 to 1992, Atmos Environ, 28, 2623–2637, https://doi.org/10.1016/1352-2310(94)90436-7, 1994.

Derwent, R. G., Jenkin, M. E., Saunders, S. M., and Pilling, M. J.: Photochemical ozone creation potentials for organic compounds in northwest Europe calculated with a master chemical mechanism, Atmos Environ, 32, 2429–2441, https://doi.org/10.1016/S1352-2310(98)00053-3, 1998.

779 Derwent, R. G., Collins, W. J., Johnson, C. E., and Stevenson, D. S.: Transient behaviour of
780 tropospheric ozone precursors in a global 3-d ctm and their indirect greenhouse effects, 2001.

781 Derwent, R. G., Stevenson, D. S., Collins, W. J., and Johnson, C. E.: Intercontinental transport
782 and the origins of the ozone observed at surface sites in Europe, Atmos Environ, 38, 1891–
783 1901, https://doi.org/10.1016/j.atmosenv.2004.01.008, 2004.

784 Derwent, R. G., Stevenson, D. S., Doherty, R. M., Collins, W. J., and Sanderson, M. G.: How
785 is surface ozone in Europe linked to Asian and North American NOx emissions?, Atmos
786 Environ, 42, 7412–7422, https://doi.org/10.1016/j.atmosenv.2008.06.037, 2008.

787 Derwent, R. G., Manning, A. J., Simmonds, P. G., Spain, T. G., and O'Doherty, S.: Analysis
788 and interpretation of 25 years of ozone observations at the Mace Head Atmospheric Research
789 Station on the Atlantic Ocean coast of Ireland from 1987 to 2012, Atmos Environ, 80, 361–
790 368, https://doi.org/10.1016/j.atmosenv.2013.08.003, 2013.

791 Derwent, R. G., Manning, A. J., Simmonds, P. G., and Doherty, S. O.: Long-term trends in
792 ozone in baseline and European regionally-polluted air at Mace Head , Ireland over a 30-year
793 period, Atmos Environ, 179, 279–287, https://doi.org/10.1016/j.atmosenv.2018.02.024, 2018.

794 Derwent, R. G., Parrish, D. D., Manning, A. J., Spain, T. G., Simmonds, P. G., and O'Doherty,
795 S.: Ozone at Mace Head, Ireland from 1987 to 2021: Declining baselines, phase-out of
796 European regional pollution, COVID-19 impacts, Atmos Environ, 320,
797 https://doi.org/10.1016/j.atmosenv.2023.120322, 2024.

798 Ding, J., Dai, Q., Fan, W., Lu, M., Zhang, Y., Han, S., and Feng, Y.: Impacts of meteorology
799 and precursor emission change on O3 variation in Tianjin, China from 2015 to 2021, J Environ
800 Sci (China), 126, 506–516, https://doi.org/10.1016/j.jes.2022.03.010, 2023.

Donlon, B., Cahalane, A., and Fanning, A.: Ireland's State of the Environment Report 2024 Editors, 2024.

Draxler, R. R. Evaluation of an Ensemble Dispersion Calculation. http://wesley.wwb.noaa.gov/reanalysis.html, 2003.

EEA. Trends and projections in Europe 2024. https://doi.org/10.2800/7574066, 2024.

Emmons, L. K., Hess, P. G., Lamarque, J.-F., and Pfister, G. G.: Tagged ozone mechanism for MOZART-4, CAM-chem and other chemical transport models, Atmos. Chem. Phys., **12**, 4607–4622, , https://doi.org/10.5194/acp-12-4607-2012,2012.

Finch, D. P., & Palmer, P. I., Increasing ambient surface ozone levels over the UK accompanied by fewer extreme events. Atmospheric Environment, 237, 117627, https://doi.org/https://doi.org/10.1016/j.atmosenv.2020.117627, 2020.

Fiore, A. M., Dentener, F. J., Wild, O., Cuvelier, C., Schultz, M. G., Hess, P., Textor, C., Schulz, M., Doherty, R. M., Horowitz, L. W., MacKenzie, I. A., Sanderson, M. G., Shindell, D. T., Stevenson, D. S., Szopa, S., Van Dingenen, R., Zeng, G., Atherton, C., Bergmann, D., Bey, I., Carmichael, G., Collins, W. J., Duncan, B. N., Faluvegi, G., Folberth, G., Gauss, M., Gong, S., Hauglustaine, D., Holloway, T., Isaksen, I. S. A., Jacob, D. J., Jonson, J. E., Kaminski, J. W., Keating, T. J., Lupu, A., Manner, E., Montanaro, V., Park, R. J., Pitari, G., Pringle, K. J., Pyle, J. A., Schroeder, S., Vivanco, M. G., Wind, P., Wojcik, G., Wu, S., and Zuber, A.: Multimodel estimates of intercontinental source-receptor relationships for ozone pollution, Journal of Geophysical Research Atmospheres, 114, https://doi.org/10.1029/2008JD010816, 2009.

Fowler, D., Coyle, M., Skiba, U., Sutton, M. A., Cape, J. N., Reis, S., Sheppard, L. J., Jenkins, A., Grizzetti, B., Galloway, J. N., Vitousek, P., Leach, A., Bouwman, A. F., Butterbach-Bahl, K., Dentener, F., Stevenson, D., Amann, M., and Voss, M.: The global nitrogen cycle in the

824 Twentyfirst century, Philosophical Transactions of the Royal Society B: Biological Sciences,
825 368, https://doi.org/10.1098/rstb.2013.0164, 2013.

826 Girach, I. A., Tripathi, N., Nair, P. R., Sahu, L. K., and Ojha, N.: O3 and CO in the South Asian
827 outflow over the Bay of Bengal: Impact of monsoonal dynamics and chemistry, Atmos Environ,
828 233, https://doi.org/10.1016/j.atmosenv.2020.117610, 2020.

829 Griffiths, P. T., Murray, L. T., Zeng, G., Shin, Y. M., Abraham, N. L., Archibald, A. T., Deushi,
830 M., Emmons, L. K., Galbally, I. E., Hassler, B., Horowitz, L. W., Keeble, J., Liu, J., Moeini,
831 O., Naik, V., and Connor, F. M. O.: Tropospheric ozone in CMIP6 simulations, 4187–4218,
832 2021.

833 Grigas, T., Ovadnevaite, J., Ceburnis, D., Moran, E., McGovern, F. M., Jennings, S. G., and
834 O'Dowd, C.: Sophisticated Clean Air Strategies Required to Mitigate Against Particulate
835 Organic Pollution, Sci Rep, 7, https://doi.org/10.1038/srep44737, 2017.

836 Guerreiro, C. B. B., Foltescu, V., and de Leeuw, F.: Air quality status and trends in Europe,
837 Atmos Environ, 98, 376–384, https://doi.org/10.1016/j.atmosenv.2014.09.017, 2014.

838 Huang, M., Carmichael, G. R., Pierce, R. B., Jo, D. S., Park, R. J., Flemming, J., Emmons, L.
839 K., Bowman, K. W., Henze, D. K., Davila, Y., Sudo, K., Jonson, J. E., Lund, M. T., Janssens-
840 Maenhout, G., Dentener, F. J., Keating, T. J., & Saiz-Lopez, A. (2017). Impact of
841 intercontinental pollution transport on North American ozone air pollution: An HTAP phase 2
842 multi-model study. Atmospheric Chemistry and Physics, 17(9), 5721–5750.
843 https://doi.org/10.5194/acp-17-5721-2017

844 IPCC, Masson-Delmotte, V., Zhai, P., Chen, Y., Goldfarb, L., Gomis, M. I., Matthews, J. B. R.,
845 Berger, S., Huang, M., Yelekçi, O., Yu, R., Zhou, B., Lonnoy, E., Maycock, T. K., Waterfield,
846 T., Leitzell, K., & Caud, N. Working Group I Contribution to the Sixth Assessment Report of
847 the Intergovernmental Panel on Climate Change Edited by. www.ipcc.ch, 2021.

848 Jeon, W. B., Lee, S. H., Lee, H., Park, C., Kim, D. H., and Park, S. Y.: A study on high ozone
849 formation mechanism associated with change of NOx/VOCs ratio at a rural area in the Korean
850 Peninsula, Atmos Environ, 89, 10–21, https://doi.org/10.1016/j.atmosenv.2014.02.005, 2014.

851 Jonson, J. E., Stohl, A., Fiore, A. M., Hess, P., Szopa, S., Wild, O., Zeng, G., Dentener, F. J.,
852 Lupu, A., Schultz, M. G., Duncan, B. N., Sudo, K., Wind, P., Schulz, M., Marmer, E., Cuvelier,
853 C., Keating, T., Zuber, A., Valdebenito, A., Dorokhov, V., De Backer, H., Davies, J., Chen, G.
854 H., Johnson, B., Tarasick, D. W., Stübi, R., Newchurch, M. J., Von Der Gathen, P., Steinbrecht,
855 W., and Claude, H.: A multi-model analysis of vertical ozone profiles, Atmos Chem Phys, 10,
856 5759–5783, https://doi.org/10.5194/acp-10-5759-2010, 2010.

857 Khiem, M., Ooka, R., Huang, H., Hayami, H., Yoshikado, H., and Kawamoto, Y.: Analysis of
858 the Relationship between Changes in Meteorological Conditions and the Variation in Summer
859 Ozone Levels over the Central Kanto Area, Advances in Meteorology, 2010, 1–13,
860 https://doi.org/10.1155/2010/349248, 2010.

861 Lamarque, J. F. and Solomon, S.: Impact of changes in climate and halocarbons on recent lower
862 stratosphere ozone and temperature trends, J Clim, 23, 2599–2611,
863 https://doi.org/10.1175/2010JCLI3179.1, 2010.

864 Lamarque, J. F., Kinnison, D. E., Hess, P. G., and Vitt, F. M.: Simulated lower stratospheric
865 trends between 1970 and 2005: Identifying the role of climate and composition changes,
866 Journal of Geophysical Research Atmospheres, 113, https://doi.org/10.1029/2007JD009277,
867 2008.

868 Lamarque, J. F., Bond, T. C., Eyring, V., Granier, C., Heil, A., Klimont, Z., Lee, D., Liousse,
869 C., Mieville, A., Owen, B., Schultz, M. G., Shindell, D., Smith, S. J., Stehfest, E., Van
870 Aardenne, J., Cooper, O. R., Kainuma, M., Mahowald, N., McConnell, J. R., Naik, V., Riahi,
871 K., and Van Vuuren, D. P.: Historical (1850-2000) gridded anthropogenic and biomass burning

emissions of reactive gases and aerosols: Methodology and application, Atmos Chem Phys, 10, 7017–7039, https://doi.org/10.5194/acp-10-7017-2010, 2010.

Lamarque, J. F., Emmons, L. K., Hess, P. G., Kinnison, D. E., Tilmes, S., Vitt, F., Heald, C. L., Holland, E. A., Lauritzen, P. H., Neu, J., Orlando, J. J., Rasch, P. J., and Tyndall, G. K.: CAM-chem: Description and evaluation of interactive atmospheric chemistry in the Community Earth System Model, Geosci Model Dev, 5, 369–411, https://doi.org/10.5194/gmd-5-369-2012, 2012.

Lefohn, A. S., Malley, C. S., Smith, L., Wells, B., Hazucha, M., Simon, H., Naik, V., Mills, G., Schultz, M. G., Paoletti, E., De Marco, A., Xu, X., Zhang, L., Wang, T., Neufeld, H. S., Musselman, R. C., Tarasick, D., Brauer, M., Feng, Z., Tang, H., Kobayashi, K., Sicard, P., Solberg, S., and Gerosa, G.: Tropospheric ozone assessment report: Global ozone metrics for climate change, human health, and crop/ecosystem research, Elementa, 6, https://doi.org/10.1525/elementa.279, 2018.

Lin, M., Fiore, A. M., Cooper, O. R., Horowitz, L. W., Langford, A. O., Levy, H., Johnson, B. J., Naik, V., Oltmans, S. J., and Senff, C. J.: Springtime high surface ozone events over the western United States: Quantifying the role of stratospheric intrusions, Journal of Geophysical Research Atmospheres, 117, https://doi.org/10.1029/2012JD018151, 2012.

Lin, Y., Jiang, F., Zhao, J., Zhu, G., He, X., Ma, X., Li, S., Sabel, C. E., and Wang, H.: Impacts of O_3 on premature mortality and crop yield loss across China, *Atmos. Environ.*, **194**, 41–47, https://doi.org/10.1016/j.atmosenv.2018.09.024, 2018.

Lupaşcu, A., Otero, N., Minkos, A., and Butler, T.: Attribution of surface ozone to NOx and volatile organic compound sources during two different high ozone events, Atmos Chem Phys, 22, 11675–11699, https://doi.org/10.5194/acp-22-11675-2022, 2022.

Ma

McVeigh, P., O′Dowd, C., and Berresheim, H.: Eddy Correlation Measurements of Ozone Fluxes over Coastal Waters West of Ireland, Advances in Meteorology, 2010, https://doi.org/10.1155/2010/754941, 2010.

Moiseenko, K. B., Vasileva, A. V., Skorokhod, A. I., Belikov, I. B., Repin, A. Y., and Shtabkin, Y. A.: Regional Impact of Ozone Precursor Emissions on NOX and O3 Levels at ZOTTO Tall Tower in Central Siberia, Earth and Space Science, 8, https://doi.org/10.1029/2021EA001762, 2021.

Molod, A., Takacs, L., Suarez, M., and Bacmeister, J.: Development of the GEOS-5 atmospheric general circulation model: Evolution from MERRA to MERRA2, Geosci Model Dev, 8, 1339–1356, https://doi.org/10.5194/gmd-8-1339-2015, 2015.

Monks, P. S., Archibald, A. T., Colette, A., Cooper, O., Coyle, M., Derwent, R., Fowler, D., Granier, C., Law, K. S., Mills, G. E., Stevenson, D. S., Tarasova, O., Thouret, V., Von Schneidemesser, E., Sommariva, R., Wild, O., and Williams, M. L.: Tropospheric ozone and its precursors from the urban to the global scale from air quality to short-lived climate forcer, https://doi.org/10.5194/acp-15-8889-2015, 13 August 2015.

Nalam, A., Lupaşcu, A., Ansari, T., and Butler, T.: Regional and sectoral contributions of NO_x and reactive carbon emission sources to global trends in tropospheric ozone during the 2000–2018 period, Atmos. Chem. Phys., 25, 5287–5311, https://doi.org/10.5194/acp-25-5287-2025, 2025.

Nelson, B. S., et al.: Urban ozone trends in Europe and the USA (2000–2021), Atmos. Chem. Phys., 25, 16009–16032, https://doi.org/10.5194/acp-25-16009-2025, 2025

O'Dowd, C., Ceburnis, D., Ovadnevaite, J., Vaishya, A., Rinaldi, M., and Facchini, M. C.: Do anthropogenic, continental or coastal aerosol sources impact on a marine aerosol signature at

Mace Head?, Atmos Chem Phys, 14, 10687–10704, https://doi.org/10.5194/acp-14-10687-2014, 2014.

Oltmans, S.J., Lefohn, A.S., Harris, J.M., Galbally, I., Scheel, H.E., Bodeker, G., Brunke, E., Claude, H., Tarasick, D., Johnson, B.J. and Simmonds, P.: Long-term changes in tropospheric ozone. Atmos Environ, 40(17), 3156-3173, https://doi.org/10.1016/j.atmosenv.2006.01.029. , 2006.

Oltmans, S. J., Lefohn, A. S., Shadwick, D., Harris, J. M., Scheel, H. E., Galbally, I., Tarasick, D. W., Johnson, B. J., Brunke, E. G., Claude, H., Zeng, G., Nichol, S., Schmidlin, F., Davies, J., Cuevas, E., Redondas, A., Naoe, H., Nakano, T., and Kawasato, T.: Recent tropospheric ozone changes - A pattern dominated by slow or no growth, Atmos Environ, 67, 331–351, https://doi.org/10.1016/j.atmosenv.2012.10.057, 2013.

Ordóñez, C., Garrido-Perez, J. M., & García-Herrera, R. Early spring near-surface ozone in Europe during the COVID-19 shutdown: Meteorological effects outweigh emission changes. Science of The Total Environment, 747, 141322. https://doi.org/https://doi.org/10.1016/j.scitotenv.2020.141322, 2020.

Pallé, E., and Butler, C.J.. :Comparison of sunshine records and synoptic cloud observations: a case study for Ireland." *Physics and Chemistry of the Earth, Parts A/B/C* 27.6-8: 405-414, 2002.

Pan, C., Zhu, B., Gao, J., Hou, X., Kang, H., and Wang, D.: Quantifying Arctic lower stratospheric ozone sources in winter and spring, Sci Rep, 8, https://doi.org/10.1038/s41598-018-27045-5, 2018.

Paoletti, E.: Impact of ozone on Mediterranean forests: A review, Environmental Pollution, 144, 463–474, https://doi.org/10.1016/j.envpol.2005.12.051, 2006.

942 Pausata, F. S. R., Pozzoli, L., Vignati, E., & Dentener, F. J.. North Atlantic Oscillation and
943 tropospheric ozone variability in Europe: Model analysis and measurements intercomparison.
944 Atmospheric Chemistry and Physics, 12(14), 6357–6376. https://doi.org/10.5194/acp-12-
945 6357-2012,2012.

946 Pio, C. A., Feliciano, M. S., Vermeulen, A. T., and Sousa, E. C.: Seasonal variability of ozone
947 dry deposition under southern European climate conditions, in Portugal, Atmospheric
948 Environment, 195–205 pp., 2000.

949 Russo, M. R., Kerridge, B. J., Abraham, N. L., Keeble, J., Latter, B. G., Siddans, R., Weber, J.,
950 Griffiths, P. T., Pyle, J. A., and Archibald, A. T.: Seasonal , interannual and decadal variability
951 of tropospheric ozone in the North Atlantic : comparison of UM-UKCA and remote sensing
952 observations for 2005 – 2018, 6169–6196, 2023.

953 Saiz-Lopez, A., Mahajan, A. S., Abbatt, J., Bobrowski, N., Brown, S. S., Burrows, J. P.,
954 Carpenter, L. J., Chipperfield, M. P., Cuevas, C. A., Fernandez, R., Hossaini, R., Kinnison,
955 D. E., Lamarque, J.-F., Finlayson-Pitts, B. J., Plane, J. M. C., Platt, U., Pratt, K., Ravishankara,
956 A. R., Salawitch, R. J., Saltzman, E. S., Simpson, W. R., Solomon, S., Thornton, J. A., & Wang,
957 T.: The influence of short-lived halogens on atmospheric chemistry and climate, Nature, 648,
958 289–299, https://doi.org/10.1038/s41586-025-09753-x, 2025.

959 Seinfeld, J. H. and Pandis, S. N.: Atmospheric Chemistry and Physics: From Air Pollution to
960 Climate Change, 3rd edn., Wiley, Hoboken, NJ, 2016.

961 Shindell, D. T., Chin, M., Dentener, F., Doherty, R. M., Faluvegi, G., Fiore, A. M., Hess, P.,
962 Koch, D. M., Mackenzie, I. A., Sanderson, M. G., Schultz, M. G., Schulz, M., Stevenson, D.
963 S., Teich, H., Textor, C., Wild, O., Bergmann, D. J., Bey, I., Bian, H., Cuvelier, C., Duncan, B.
964 N., Folberth, G., Horowitz, L. W., Jonson, J., Kaminski, J. W., Marmer, E., Park, R., Pringle,
965 K. J., Schroeder, S., Szopa, S., Takemura, T., Zeng, G., Keating, T. J., and Zuber, A.:

966 Atmospheric Chemistry and Physics A multi-model assessment of pollution transport to the
967 Arctic, Atmos. Chem. Phys, 5353–5372 pp., 2008.

968 Sicard, P., Serra, R., and Rossello, P.: Spatiotemporal trends in ground-level ozone
969 concentrations and metrics in France over the time period 1999-2012, Environ Res, 149, 122–
970 144, https://doi.org/10.1016/j.envres.2016.05.014, 2016.

971 Simmonds, P. G. and Derwent, R. G. :Measurements of ozone and other radiatively active gases
972 at Mace Head in the Republic of Ireland, Atmos Environ, 25A(9), 1795-1808, 1991.

973 Simmonds, P. G., Derwent, R. G., Manning, A. L., and Spain, G.: Significant growth in surface
974 ozone at Mace Head, Ireland, 1987-2003, Atmos Environ, 38, 4769–4778,
975 https://doi.org/10.1016/j.atmosenv.2004.04.036, 2004.

976 Soares, J., UBA, D. P., UBA, S. K., EEA, A. G. O., EEA, A. G., & Horálek, J. Health Risk
977 Assessment of Air Pollution: assessing the environmental burden of disease in Europe in 2021.
978 ETC HE Report, 7, 104, 2023.

979 Spohn, T. K., Martin, D., Geever, M., and O'Dowd, C.: Effect of COVID-19 lockdown on
980 regional pollution in Ireland, Air Qual Atmos Health, 15, 221–234,
981 https://doi.org/10.1007/s11869-021-01098-4, 2022.

982 Stein, A. F., Draxler, R. R., Rolph, G. D., Stunder, B. J. B., Cohen, M. D., and Ngan, F.: NOAA's
983 HYSPLIT atmospheric transport and dispersion modeling system, Bulletin of the American
984 Meteorological Society, 96, 2059–2077, 2015, https://doi.org/10.1175/BAMS-D-14-00110.1.

985 Stunder, B.J.B.: Global Data Assimilation System (GDAS) Archive Information, NOAA Air
986 Resources Laboratory, Silver Spring, MD, USA, December 1, 2004.

Sudo, K., and H. Akimoto, H.: Global source attribution of tropospheric ozone: Long-range transport from various source regions, J. Geophys. Res., 112, D12302, doi:10.1029/2006JD007992, 2007.

Tan, J., Fu, J. S., Dentener, F., Sun, J., Emmons, L., Tilmes, S., Flemming, J., Takemura, T., Bian, H., Zhu, Q., Yang, C. E., and Keating, T.: Source contributions to sulfur and nitrogen deposition - An HTAP II multi-model study on hemispheric transport, Atmos Chem Phys, 18, 12223–12240, https://doi.org/10.5194/acp-18-12223-2018, 2018.

Tavella, R. A. and da Silva Júnior, F. M. R.: Watch out for trends: did ozone increased or decreased during the COVID-19 pandemic?, Environmental Science and Pollution Research, 28, 67880–67885, https://doi.org/10.1007/s11356-021-17142-w, 2021.

Tilmes, S., Sanderson, B. M., and O'Neill, B. C.: Climate impacts of geoengineering in a delayed mitigation scenario, Geophys Res Lett, 43, 8222–8229, https://doi.org/10.1002/2016GL070122, 2016.

Tilmes, S., Lamarque, J. F., Emmons, L. K., Kinnison, D. E., Ma, P. L., Liu, X., Ghan, S., Bardeen, C., Arnold, S., Deeter, M., Vitt, F., Ryerson, T., Elkins, J. W., Moore, F., Spackman, J. R., and Val Martin, M.: Description and evaluation of tropospheric chemistry and aerosols in the Community Earth System Model (CESM1.2), Geosci Model Dev, 8, 1395–1426, https://doi.org/10.5194/gmd-8-1395-2015, 2015.

Todorović, M. N., Radenković, M. B., Rajšić, S. F., & Ignjatović, L. M. Evaluation of mortality attributed to air pollution in the three most populated cities in Serbia. International Journal of Environmental Science and Technology, 16(11), 7059–7070. https://doi.org/10.1007/s13762-019-02384-6, 2019.

Tripathi, O. P., Jennings, S. G., O'Dowd, C. D., Coleman, L., Leinert, S., O'Leary, B., Moran, E., O'Doherty, S. J., and Spain, T. G.: Statistical analysis of eight surface ozone measurement

1011 series for various sites in Ireland, Journal of Geophysical Research Atmospheres, 115, 1–20,
1012 https://doi.org/10.1029/2010JD014040, 2010.

1013 Tripathi, O. P., Jennings, S. G., O'Dowd, C., O'Leary, B., Lambkin, K., Moran, E., O'Doherty,
1014 S. J., and Gerard Spain, T.: An assessment of the surface ozone trend in Ireland relevant to air
1015 pollution and environmental protection, Atmos Pollut Res, 3, 341–351,
1016 https://doi.org/10.5094/APR.2012.038, 2012.

1017 Tripathi, O. P., Jennings, S. G., Colman, L., Lambkin, K., Moran, E., and Dowd, C. O.: Ozone
1018 levels , changes and trends over Ireland – an Integrated Analysis, 2013.

1019 Tripathi, O. P., Gerard Jennings, S., Colman, L., Lambkin, K., and Moran, E.: EPA STRIVE
1020 Programme 2007-2013 Ozone levels, changes and trends over Ireland-an Integrated Analysis
1021 (2006-AQ-MS-50) STRIVE Report, n.d.

1022 Tripathi, R. M., Vinod Kumar, A., Manikandan, S. T., Bhalke, S., Mahadevan, T. N., and
1023 Puranik, V. D.: Vertical distribution of atmospheric trace metals and their sources at Mumbai,
1024 India, Atmos Environ, 38, 135–146, https://doi.org/10.1016/j.atmosenv.2003.09.006, 2004.

1025 Vautard, R., Moran, M. D., Solazzo, E., Gilliam, R. C., Matthias, V., Bianconi, R., Chemel, C.,
1026 Ferreira, J., Geyer, B., Hansen, A. B., Jericevic, A., Prank, M., Segers, A., Silver, J. D.,
1027 Werhahn, J., Wolke, R., Rao, S. T., and Galmarini, S.: Evaluation of the meteorological forcing
1028 used for the Air Quality Model Evaluation International Initiative (AQMEII) air quality
1029 simulations, Atmos Environ, 53, 15–37, https://doi.org/10.1016/j.atmosenv.2011.10.065, 2012.

1030 Van Der Werf, G. R., Randerson, J. T., Giglio, L., Collatz, G. J., Mu, M., Kasibhatla, P. S.,
1031 Morton, D. C., Defries, R. S., Jin, Y., and Van Leeuwen, T. T.: Global fire emissions and the
1032 contribution of deforestation, savanna, forest, agricultural, and peat fires (1997-2009), Atmos
1033 Chem Phys, 10, 11707–11735, https://doi.org/10.5194/acp-10-11707-2010, 2010.

1034 Wespes, C., Hurtmans, D., Clerbaux, C., and Coheur, P. F.: O3 variability in the troposphere as
1035 observed by IASI over 2008-2016: Contribution of atmospheric chemistry and dynamics, J
1036 Geophys Res, 122, 2429–2451, https://doi.org/10.1002/2016JD025875, 2017.

1037 WHO. Global Air Quality Guidelines: Particulate Matter (PM2.5 and PM10), Ozone, Nitrogen
1038 Dioxide, Sulfur Dioxide and Carbon Monoxide (World Health Organization, 2021.

1039 Wild, O. & Ryan, E. M.: Quantifying and addressing the uncertainties in tropospheric ozone
1040 and OH in a global chemistry transport model, EGUsphere [preprint],
1041 https://doi.org/10.5194/egusphere-2025-4534, 2025.

1042 Yan, Y., et al.: Analysis of European ozone trends in the period 1995–2014, Atmos. Chem.
1043 Phys., 18, 5589–5605, https://doi.org/10.5194/acp-18-5589-2018, 2018.

1044 Yerramilli, A., Srinivas Challa, V., Rao Dodla, V. B., Myles, L. T., Pendergrass, W. R., Vogel,
1045 C. A., Tuluri, F., Baham, J. M., Hughes, R., Patrick, C., Young, J., & Swanier, S. Simulation of
1046 surface ozone pollution in the Central Gulf Coast region during summer synoptic condition
1047 using WRF/Chem air quality model. Atmospheric Pollution Research, 3(1), 55–71.
1048 https://doi.org/10.5094/APR.2012.005,2012.

1049 Young, P. J., Archibald, A. T., Bowman, K. W., Lamarque, J., Naik, V., Stevenson, D. S., and
1050 Tilmes, S.: Pre-industrial to end 21st century projections of tropospheric ozone from the
1051 Atmospheric Chemistry and Climate Model Intercomparison Project (ACCMIP), 2063–2090,
1052 https://doi.org/10.5194/acp-13-2063-2013, 2013.

1053 Yu, H., Chin, M., West, J. J., Atherton, C. S., Bellouin, N., Bergmann, D., Bey, I., Bian, H.,
1054 Diehl, T., Forberich, O., Hess, P., Schulz, M., Takemura, T., & Tan, Q.. A multimodel
1055 assessment of the influence of regional anthropogenic emission reductions on aerosol direct
1056 radiative forcing and the role of intercontinental transport. Journal of Geophysical Research:
1057 Atmospheres, 118(13), 7004–7025. https://doi.org/10.1002/jgrd.50502,2013.

Zhang, J. J., Wei, Y., & Fang, Z. Ozone pollution: A major health hazard worldwide. Frontiers in Immunology, 10(OCT), 1–10. https://doi.org/10.3389/fimmu.2019.02518,2019.

Zhang, C. and Stevenson, D.: Characteristic changes of ozone and its precursors in London during COVID-19 lockdown and the ozone surge reason analysis, Atmos. Environ., **273**, 118980, https://doi.org/10.1016/j.atmosenv.2022.118980,2022

Zhu, T., Melamed, M., Parrish, D., Gauss, M., Klenner, L. G.,Lawrence, M., Konare, A., and Liousse, C.: Impacts of Megacities on Air Pollution and Climate, WMO, Geneva, 2012.

Figure Captions

Figure 1. The map of EPA O_3 measurement sites over Ireland with classification of backgrounds.

Figure 2. Annual average O_3 concentration at different sites in Ireland. In each box, the lowest whisker level represents the 5^{th} percentile, the box spans from the 25^{th} to the 75^{th} percentile, the horizontal line within the box represents the median 50th percentile, and the upper whisker represents the 95^{th} percentile. The average of monthly O_3 values calculated for the entire period of each station, and the red line shows the average monthly O_3 variation of all sites top axis shows the month (1– 12).

Figure 3. Monthly trend analysis of O_3 at different sites for 10 year period. (2012-2022) Adopting the trend reliability scale defined for TOAR-II studies (Chang et al., 2023), trends with very high certainty are marked by ***($p \leq 0.001$), , trends with high certainty with **($p \leq 0.01$), and low to medium certainty with **($p \leq 0.05$). Positive trends are in red shade and negative trends are in blue shade.

Figure 5.- Trend in O_3 precursors NO_2 (a), and CH4 (b) at different sites. Trends with very high certainty are marked by ***($p \leq 0.001$), , trends with high certainty with **($p \leq 0.01$),, and low to medium certainty with *($p \leq 0.05$).

Figure 6. Percentage change in NO_2 and O_3 during the lockdown period of 2020 as compared to the 2017-2019 average at different sites in Ireland for (a) March, (b) April, (c) May Month.

Figure 7. The comparison of Monthly CAM4 – Chem O_3 and Monthly O_3 observations at five sites in Ireland.

Figure 8. Absolute contribution of major NOx sources (a) (NOx Tagging) and VOC source (b) (NOx Tagging) to the CAM4-Chem simulated surface O_3 for the Mace Head grid cell between 2000-2018.

Figure 9. Trends in contributions to the monthly average modelled Mace Head grid cell surface O3 at for the 2000-2018 period derived from (a) NO_x tagging and (b)VOC tagging.

Figure 10. Trend in seasonal Average of observed O3 (black) and Model O_3 (red) at Mace Head, separated into the clean sector and EU-influenced sector.

Figure 11. Exceedances measured at Mace Head per month from 2000 until 2022, during the clean air sector(green) and EU influenced sector (yellow). The percentage of both to total exceedances is shown in the inlay.

Figure 12. (a) The trend in Spring-time exceedances measured at Mace Head between 2000 and 2022 (blue) with the clean-air exceedances (gold), and (b) The trend in 95th percentile of spring (Mar- May) O_3 measured in $\mu g /m^3$ for the clean sector (blue) and the EU-influenced sector (gold).

Figure 13 Monthly cumulative Mace Head grid cell O_3 contributions to EU influenced sector and clean sector exceedances (a) NOx tagging and (b) VOC tagging Mace Head grid cell.

Chang, K.-L., Schultz, M. G., Koren, G., & Selke, N. (2023). Guidance note on best statistical practices for TOAR analyses. *arXiv preprint arXiv:2304.14236*.

EEA. (2024). *Exceedance of air quality standards in Europe* (Indicator AIR003, Issue. https://www.eea.europa.eu/en/analysis/indicators/exceedance-of-air-quality-standards

Soares, J., UBA, D. P., UBA, S. K., EEA, A. G. O., EEA, A. G., & Horálek, J. (2023). Health Risk Assessment of Air Pollution: assessing the environmental burden of disease in Europe in 2021. *ETC HE Report*, *7*, 104.

World Health, O. (2021). *WHO global air quality guidelines: particulate matter (PM2.5 and PM10), ozone, nitrogen dioxide, sulfur dioxide and carbon monoxide*. World Health Organization. https://iris.who.int/handle/10665/345329